

Fused Potts Models

W.M.Koo¹ and H.Saleur²

Department of Physics, Yale University
P O Box 6666
New Haven, CT 06511, USA

Abstract

Generalizing the mapping between the Potts model with nearest neighbour interaction and the six vertex model, we build a family of "fused Potts models" related to the spin $k/2$ $U_q\text{su}(2)$ invariant vertex model and quantum spin chain. These Potts models have still variables taking values $1, \dots, Q$ ($\sqrt{Q} = q + q^{-1}$) but they have a set of complicated multi spin interactions. The general technique to compute these interactions, the resulting lattice geometry, symmetries, and the detailed examples of $k = 2, 3$ are given.

For $Q > 4$ spontaneous magnetizations are computed on the integrable first order phase transition line, generalizing Baxter's results for $k = 1$.

For $Q \leq 4$, we discuss the full phase diagram of the spin one ($k = 2$) anisotropic and $U_q\text{su}(2)$ invariant quantum spin chain (it reduces in the limit $Q = 4$ ($q = 1$) to the much studied phase diagram of the isotropic spin one quantum spin chain). Several critical lines and massless phases are exhibited. The appropriate generalization of the Valence Bond State method of Affleck et al. is worked out.

¹Work supported in part by DOE grant DE-AC02-76ERO3075

²Work supported in part by DOE contract DE-AC02-76ERO3075 and by the Packard foundation. Address after January 1993: Dept. of Physics and Dept. of Mathematics, USC, University Park, Los Angeles CA 90089

1 Introduction

Numerous families of integrable lattice models have recently been exhibited. In general, these families obey the following pattern. One starts with an algebra like $sl(n)$ and one of its representation say ρ . Using quantum group technology a solution of the Yang Baxter equation acting in $\rho \otimes \rho$ can be found, which encodes the Boltzmann weights of a **vertex model**. These weights are trigonometric and they depend on the quantum group deformation parameter q and the spectral parameter. The degrees of freedom are the weights of the representation ρ , and they sit on edges of usually the square lattice. Using the quantum group symmetry the model can also be reformulated as a **solid on solid model** whose degrees of freedom are highest weights and sit now on the vertices of usually the square lattice. For q a root of unity, the model truncates and a restricted sos model can be defined.

In the particular case of $su(2)$ spin $1/2$, there exists, besides the six vertex and sos model, a third "equivalent" model, the **Potts model** [1]. Its existence and relations with the first two have a precise meaning in terms of Temperley Lieb algebra representation theory. The purpose of this paper is to show that for higher spin, there is also a Potts model naturally associated with the vertex and sos models. This model still uses the same set of variables $\sigma = 1, \dots, Q$ but involves interactions that are more complicated than the nearest neighbour coupling of the spin $1/2$ case. That such models exist has been known in principle for a long time [19] but their precise definition, and the general algebraic formalism to build them, are new to the best of our knowledge. While we were working on that construction, we became aware of the work of Nienhuis [4] where the first member of the hierarchy, a Potts model with nearest and next to nearest neighbors interactions related to spin 1, has already been exhibited. However the techniques used in [4] and in our work are very different.

The construction of what we shall call Γ_k **Potts model** is discussed in details in section 3, after elementary reminders about $k = 1$ are given in section 2. From another perspective, it gives an interesting light to the differences between integer and half integer vertex models or quantum spin chains (we can in particular reformulate the spin $k/2$ $su(2)$ spin chains problems in terms of $Q = 4$ states Potts models). For k greater than one, only submanifolds of the full parameter space are integrable. In section 4 we discuss the simplest integrable line for $Q > 4$ where a first order phase transition takes place. We compute spontaneous magnetizations by generalizing Baxter's calculation for spin $1/2$.

We discuss in section 5 the full phase diagram of the $k = 2$ model, mainly in terms of the corresponding one dimensional quantum spin chain. This phase diagram restricts in the case $Q = 4$ to the widely studied one for the spin 1 $su(2)$ hamiltonian. Critical properties are studied with particular emphasis on the integrable lines. We also construct the valence bond states for the P_2 projector for arbitrary Q thereby extending the construction in [7] to anisotropic systems (with quantum group symmetry). In opposition to [7], phase transitions are encountered as Q varies.

Two appendices are included. Appendix A contains the explicit expression for the Boltzmann weights of the $k = 3$ Potts model. Various loop model interpretations for the family of Potts model, in particular for $k = 2$, are reviewed briefly in appendix B.

2 The Q -state Potts model and staggered six-vertex model

We begin by reviewing the Q -state Potts model on a square lattice. We consider a cylinder made of an $l \times t$ rectangular strip \mathcal{L} with free boundary condition on the top and bottom rows, and periodic in the time direction. The partition function of the model with horizontal and vertical couplings K_1 and K_2 is given by[1]

$$Z_{\text{Potts}} = \sum_{\{\sigma_i\}} \prod_{\langle ij \rangle} e^{K_1 \delta_{\sigma_i, \sigma_j} + K_2 \delta_{\sigma_i, \sigma_j}} , \quad (2.1)$$

where the product is over all neighboring horizontal and vertical links $\langle ij \rangle$ and σ_i assumes values 1 to Q .

The column to column transfer matrix τ_{Potts} can be expressed as a product of local transfer matrices X_{2i-1} and X_{2i} which add, respectively, a horizontal and a vertical link to the lattice. We have

$$\tau_{\text{Potts}} = Q^{l/2} \prod_{i=1}^l X_{2i-1} \prod_{i=1}^l X_{2i} \quad (2.2)$$

and

$$Z_{\text{Potts}} = \text{tr}(\tau)^t \quad (2.3)$$

with

$$\begin{aligned} X_{2i-1} &= x_1 + e_{2i-1} , \\ X_{2i} &= 1 + x_2 e_{2i} , \end{aligned} \quad (2.4)$$

where we define

$$x_k = \frac{e^{K_k - 1}}{Q^{1/2}} \quad \text{for } k = 1, 2$$

and the operators e_i 's which propagate $\{\sigma_i\}$ to $\{\sigma'_i\}$ in the time direction, have matrix elements given by[8]

$$\begin{cases} (e_{2i})_{\sigma, \sigma'} &= Q^{1/2} \delta_{\sigma_i, \sigma_{i+1}} \prod_{j=1}^l \delta_{\sigma_j, \sigma'_j} , \\ (e_{2i-1})_{\sigma, \sigma'} &= Q^{-1/2} \prod_{j \neq i} \delta_{\sigma_j, \sigma'_j} , \end{cases} \quad (2.5)$$

They satisfy the following relations (dropping the subscripts from now on)

$$\begin{cases} e_i^2 &= Q^{1/2} e_i , \\ e_i e_{i \pm 1} e_i &= e_i , \\ [e_i, e_j] &= 0 \quad ; |i - j| \geq 2 . \end{cases} \quad (2.6)$$

The algebra generated by them is known as the Temperley Lieb algebra. In the Potts representation the following trace properties hold[9]

$$\begin{aligned} \text{tr} [w(1, e_1, \dots, e_{i-1}) e_i] &= Q^{-1/2} \text{tr} w(1, e_1, \dots, e_{i-1}) , \\ \text{tr} (e_i) &= Q^{-1/2} \text{tr} \mathbf{1} , \quad \text{and} \\ \text{tr} \mathbf{1} &= Q^l , \end{aligned} \quad (2.7)$$

where w is any word in $1, e_1, \dots, e_{i-1}$. The Potts model exhibits a duality transformation implemented by rewriting the local transfer matrices as follows

$$\begin{aligned} X_{2i-1} &= x_1(1 + x_1^{-1}e_{2i-1}), \\ X_{2i} &= x_2(x_2^{-1} + e_{2i}), \end{aligned} \quad (2.8)$$

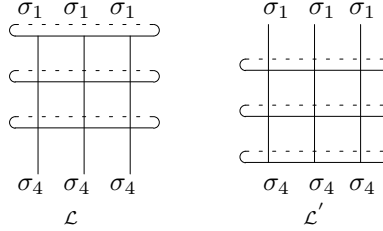
and interchanging the roles of e_{2i-1} and e_{2i} ;

$$\begin{cases} (e_{2i})_{\sigma, \sigma'} &= Q^{-1/2} \prod_{j \neq i} \delta_{\sigma_j \sigma'_j}, \\ (e_{2i-1})_{\sigma, \sigma'} &= Q^{1/2} \delta_{\sigma_i \sigma_{i+1}} \prod_{j=1}^l \delta_{\sigma_j \sigma'_j}, \end{cases} \quad (2.9)$$

which amounts to redefining X_{2i-1} and X_{2i} to be the local operators that add a vertical and a horizontal link to the Potts lattice respectively. This alternative interpretation of the roles of e_{2i-1} and e_{2i} does not alter the algebraic relations satisfied by them. We thus have

$$Z_{\text{Potts}}(x_1, x_2) = (x_1 x_2)^{lt} Z'_{\text{Potts}}(x_2^{-1}, x_1^{-1}) \quad (2.10)$$

where the prime denotes the dual lattice \mathcal{L}' which differs from \mathcal{L} by boundary effects only. (see fig.(1))



Figure(1) Geometry of the lattice and its dual

The duality transformation

$$x_1 \longleftrightarrow x_2^{-1} \quad (2.11)$$

relates high temperature to low temperature phase. Ignoring the difference in the boundary, the model is self-dual at

$$x_1 x_2 = 1, \quad (2.12)$$

and by standard argument[1] this is a line of phase transition (first order for $Q > 4$, and second order for $Q \leq 4$).

It is well known that the model can be mapped to the six-vertex (referred to as Γ_1 here) model by assigning arrows on the surrounding polygons of the clusters formed by Potts variables σ_i that have the same colors [1, 3] in the high temperature expansion. The procedure is more transparent from an algebraic point of view. Consider the tensor product of $2l$ copies of spin- $\frac{1}{2}$ representations of $U_{qsl}(2)$, then e_i can be represented in this vector space as

$$e_i = \mathbf{1} \otimes \dots \otimes \begin{pmatrix} 0 & 0 & 0 & 0 \\ 0 & q^{-1} & -1 & 0 \\ 0 & -1 & q & 0 \\ 0 & 0 & 0 & 0 \end{pmatrix} \otimes \dots \otimes \mathbf{1} \in \mathbf{C}^{\otimes 2l}, \quad (2.13)$$

where the matrix is proportional to the spin-0 projector of the i^{th} and $(i+1)^{\text{th}}$ spin- $\frac{1}{2}$ representation, it is easy to verify that the above indeed satisfies (2.6) with

$$Q^{1/2} = q + q^{-1} ,$$

and the trace properties (2.7) can be reproduced by introducing the Markov trace defined as

$$\left\{ \begin{array}{l} \text{tr} \left[q^{2S^Z} w(1, e_1, \dots, e_{i-1}) e_i \right] = (q + q^{-1})^{-1} \text{tr} \left[q^{2S^Z} w(1, e_1, \dots, e_{i-1}) \right] , \\ \text{tr} \left(q^{2S^Z} e_i \right) = (q + q^{-1})^{-1} \text{tr} \left(q^{2S^Z} \mathbf{1} \right) , \\ \text{tr} \left(q^{2S^Z} \mathbf{1} \right) = (q + q^{-1})^{2l} , \end{array} \right. \quad (2.14)$$

where

$$S^Z = \sum_{i=1}^{2l} \sigma_i^Z$$

and

$$\sigma_i^Z = \mathbf{1} \otimes \dots \otimes \left(\begin{array}{cc} \frac{1}{2} & 0 \\ 0 & -\frac{1}{2} \end{array} \right) \otimes \dots \otimes \mathbf{1} .$$

The operator X_i , with e_i given as (2.13), defines the vertex interaction of the staggered six-vertex model, that is its matrix elements encode the Boltzmann weights of the vertices with various colors for incoming and outgoing lines. The partition function is then given by

$$Z_{\text{vertex}} = \text{tr} \left(q^{2S^Z} \tau_{\text{vertex}} \right) , \quad (2.15)$$

$$\tau_{\text{vertex}} = (q + q^{-1})^l \prod_{i=1}^l X_{2i-1} \prod_{i=1}^l X_{2i} , \quad (2.16)$$

with e_i 's in the above defined by (2.13). Because of the same trace properties of the two representations, Z_{vertex} and Z_{Potts} are equal for integer Q . However, the former is defined as well for Q real (and coincides with the geometrical definition based on high temperature expansion). The Temperley Lieb generators commute with $U_q\text{sl}(2)$, so the six-vertex model has $U_q\text{sl}(2)$ symmetry. The mapping between vertex and Potts models is not one to one when q is a root of unity due to the boundary operator q^{2S^Z} in the trace and the quantum group symmetry. It is actually one to one between the Potts model and only the subset of type II representations of $U_q\text{sl}(2)$ provided by the six-vertex model[11, 12].

3 Potts model formulation of the Γ_k vertex model

3.1 The fusion procedure and mapping to Potts model

We shall construct a family of Potts models which are related to the $U_q\text{su}(2)$ invariant vertex models based on spin- $\frac{k}{2}$. We call the latter **Γ_k vertex models**. This name is non standard, and we do not know any more standard name to use instead (in [13] Γ_k refers to the number of allowed vertices, 6 for $k = 1$, 19 for $k = 2, \dots$). For the moment we therefore decide only about the symmetry, not the particular set

of interactions. The construction uses then ideas of the "fusion procedure" [5] (properly generalized) to reexpress each $U_q\text{su}(2)$ spin- $k/2$ in terms of k copies of spin- $1/2$. A pairs of such $1/2$ spins interact at vertices of the six-vertex model (Γ_1 vertex model). Each such vertex is then translated into a Potts model interaction using the results of section 2. This provides finally a Potts model with complicated inhomogeneous interactions which we call the **Γ_k Potts model**.

This construction is best explained by explicit computation. First, the Boltzmann weights of a particular vertex with two incoming and two outgoing legs carrying $U_q\text{su}(2)$ spin- $k/2$ variables are encoded in a matrix which we call for simplicity the Γ_k vertex as well. It is an operator that acts on $\mathbf{C}^{k+1} \otimes \mathbf{C}^{k+1}$. The corresponding spin- $\frac{k}{2}$ irreducible representations can be obtained from the q -symmetric tensor product of k copies of the spin- $\frac{1}{2}$ one. This is conveniently done using the q -symmetrizer defined by[14]

$$S_k = \frac{q^{k(k-1)/2}}{[k]_q!} \sum_{\sigma} q^{-|I_{\sigma}|} \prod_{i \in I_{\sigma}} s(i), \quad (3.1.1)$$

where

$$s(i) = q^{-1}\mathbf{1} - e_i.$$

In the above formula, I_{σ} denotes the collections of indices in the nonreducible decomposition of the symmetric group element σ in terms of transposition of neighbors $\tau_{i,i+1}$, $|I_{\sigma}|$ indicates the cardinality of the collections and we also introduced the q -factorial where

$$\begin{aligned} [n]_q! &= (n)_q(n-1)_q \dots (1)_q \\ \text{and } (n)_q &= \frac{q^n - q^{-n}}{q - q^{-1}}. \end{aligned} \quad (3.1.2)$$

The symmetrizer can alternatively be written recursively as[17, 18]

$$S_k = S_{k-1} \left(1 - \frac{(k-1)_q}{(k)_q} e_{k-1} \right) S_{k-1}, \quad (3.1.3)$$

which expresses S_k solely in terms of products of Γ_1 vertices.

The Γ_k vertex written in terms of Γ_1 reads then

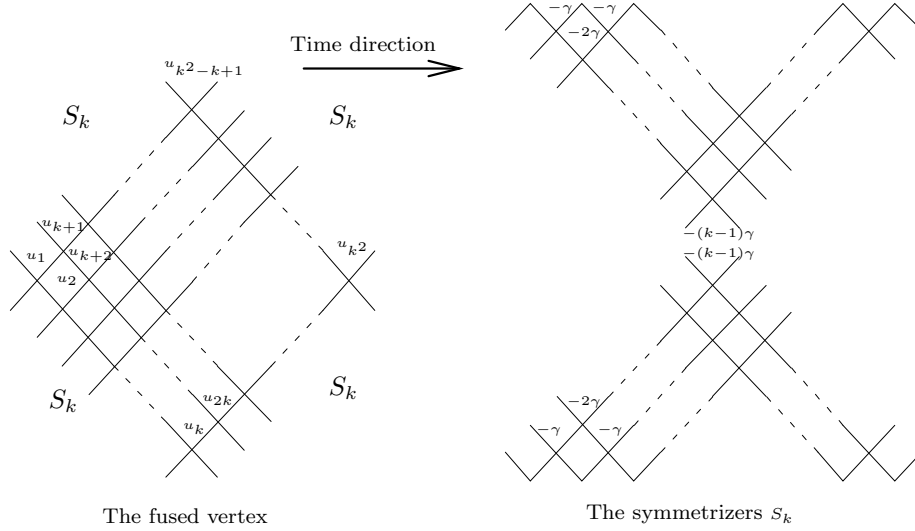
$$S_k S_k [r_k(u_1) r_{k+1}(u_2) \dots r_{2k-1}(u_k)] [r_{k-1}(u_{k+1}) \dots r_{2k-2}(u_{2k})] \dots [r_1(u_{k^2-k+1}) \dots r_k(u_{k^2})] S_k S_k, \quad (3.1.4)$$

where the first and last two S_k 's act respectively on the two in- and out- states, and we encoded the Γ_1 weights in the matrix

$$r_i(u_j) = \mathbf{1} + \frac{\sin u_j}{\sin(\gamma - u_j)} e_i \quad (3.1.5)$$

with $q = e^{i\gamma}$. Note that $r_i(u_j)$ is identical with the local operator X_i introduced in the previous section. The construction (3.1.4) is illustrated graphically in fig.(2), which shows that the interaction between the two spin- $\frac{k}{2}$ states is replaced by the interactions $r_k(u_1), \dots, r_k(u_{k^2})$ between $2k$ spin- $\frac{1}{2}$ states. It is not difficult to see that the operator (3.1.4) has $U_q\text{su}(2)$ symmetry since each of the Γ_1 vertices regarded as an operator in $\mathbf{C}^{k+1} \otimes \mathbf{C}^{k+1}$ also has $U_q\text{su}(2)$ symmetry. This together with the fact that S_k 's project onto the spin- $\frac{k}{2}$ irreducible representation, implies that the operator (3.1.4) is indeed a Γ_k vertex. It can therefore

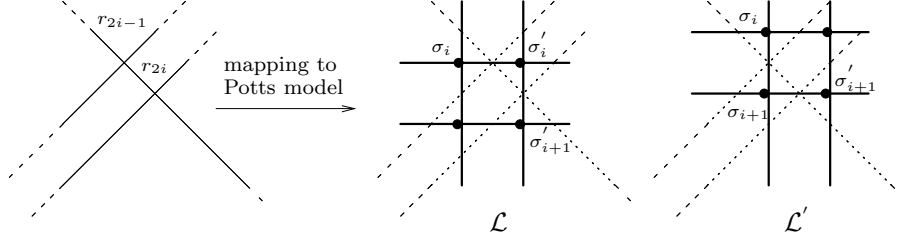
be written as a linear combination of the projectors P_j , $j = 0, 1, \dots, k$. Conversely it can be shown (see also appendix B) that any Γ_k vertex weight can be written as the above using a particular set of u_i 's. The number of independent parameters for the Γ_k vertex is equal to k (we factored out an irrelevant overall scale), which is much less than the number of u_i 's. But these are the most convenient parameters.



Figure(2) The fused Γ_k vertex; The parameters $u_1, \dots, u_{k+1}, \dots, u_{2k}, \dots$ appearing in the figure are associated with the Γ_1 vertices that make up the Γ_k vertex. The four S_k 's that act on the in- and out- states are shown on the rhs.

Next, having written the Γ_k vertex in terms of Γ_1 vertices and thus the Temperley-Lieb generators, we can use the various realizations of the Temperley-Lieb algebra. In particular, we shall consider the Potts model realization, which produces the Γ_k Potts model we set out to construct. The Potts model lattice corresponding to the Γ_k vertex is built up as follows: To each Γ_1 vertex r_i in (3.1.4), we substitute the expression (2.5) or (2.9), and call the operator (3.1.4) in this representation $\mathbf{W}(\mathbf{u})$, and the matrix elements of $W(u)$ induced by the in- and out- states of the vertex will become the Boltzmann weights of the Γ_k Potts model. Graphically we assign either a horizontal or vertical link to each spin- $\frac{1}{2}$ vertex r_j as shown in fig.(3), $W(u)$ therefore corresponds to an operator that acts on k or $k+1$ **Potts variables**, and is represented graphically as a connected collection of horizontal and vertical links, which shall be referred to as the **fundamental block** \mathcal{G}_k hereafter. The lattice \mathcal{L} is then constructed by replacing all the Γ_k vertices by these fundamental blocks. we shall elaborate on this point in next few sections. Note that there are exactly two possible mappings to the Potts model links which originate from the two possible choices of assigning links to the generator, namely (2.5) and (2.9). When (2.5) is used, a horizontal (vertical) link is associated to r_j with odd (even) subscript, whereas when (2.9) is used, the roles of vertical and horizontal links are reversed. We shall denote these two choices of mapping as **convention A and B** respectively. It will be shown that they are related by duality transformation which is inherited from that of the Γ_1 Potts model. The relation between the Γ_k vertex and Potts models generalizes that of the $k = 1$ case. In particular,

for the vertex model whose lattice has the geometry of a cylinder with periodic time boundary condition, the partition function defined as in (2.15) is equal to that of the corresponding Potts model when Q is an integer. The Markov trace in (2.15) again restricts the domain of the mapping to type II representations of $U_q\mathfrak{su}(2)$ provided by the vertex model.



Figure(3) Mapping of the Γ_1 vertices to Potts model links. In the first figure on the rhs, $r_{2i-1}(r_{2i})$ is replaced by the horizontal (vertical) Potts model links that connects σ_i and σ_{i+1} (σ'_i and σ'_{i+1}), the dual Potts model is given by the second figure on the rhs where the above vertex is mapped to a vertical (horizontal) links connecting σ_i and σ_{i+1} (σ_{i+1} and σ_{i+1})

3.2 The local interaction and its dual

We shall first work out explicitly the weight $W(u)$ for $k = 2$ and 3, and construct graphically the Potts model representation of $W(u)$, ie. the fundamental blocks \mathcal{G}_2 and \mathcal{G}_3 . The construction of the fundamental block is then generalized to arbitrary k .

For $k = 2$, the vertex is

$$r_1(-\gamma)r_3(-\gamma)r_2(u_1)r_3(u_2)r_1(u_3)r_2(u_4)r_1(-\gamma)r_3(-\gamma) , \quad (3.2.1)$$

where $r_1(-\gamma)$ is the symmetrizer S_2 . Substituting (3.1.5) into the above, we obtain a sum of products of Temperley-Lieb generators e_i , $i = 1, 2, 3$. Mapping to Potts model is done by replacing e_i 's with (2.5) or (2.9), ie. convention A or B (see fi.(4)).

With convention A, the corresponding operator in the Potts language has matrix elements

$$W_{abcd}(u) = \sum_{\alpha,\beta,\gamma,\delta} S_{a\alpha}S_{b\beta} \left(1 + Q^{1/2}x_1\delta_{\alpha\beta}\right) \left(Q^{-1/2}x_2 + \delta_{\alpha\gamma}\right) \left(Q^{-1/2}x_3 + \delta_{\beta\delta}\right) \left(1 + Q^{1/2}x_4\delta_{\gamma\delta}\right) S_{\gamma c}S_{\delta d} , \quad (3.2.2)$$

where a, b, \dots are Potts model variables taking values from 1 to Q ,

$$x_i = \frac{\sin u_i}{\sin(\gamma - u_i)}$$

and

$$S_{\alpha\beta} = -Q^{-1} + \delta_{\alpha\beta}$$

is the symmetrizer S_2 in the Potts model language. Using the fact that

$$\sum_{\beta} S_{\alpha\beta} = 0 ,$$

the weight W can be simplified as

$$W_{abcd}(f_0, f_1) = S_{ac}S_{bd} + f_0S_{ab}S_{cd} + \sum_{\alpha} Q^{1/2} f_1 S_{a\alpha}S_{b\alpha}S_{\alpha c}S_{\alpha d} \quad (3.2.3)$$

with

$$\begin{aligned} f_0 &= x_1x_2x_3x_4 , \\ f_1 &= x_1 + x_4 + x_1x_4 (Q^{1/2} + x_2 + x_3) . \end{aligned} \quad (3.2.4)$$

The three terms in the above expression have origin in the geometrical description of the Γ_2 model[15]. They correspond to the weights of the strand configurations shown in fig.(B1)(see appendix B). More precisely, the algebra generated by the corresponding operators is identical to that obtained from the strand configurations with algebraic multiplication given by appending one picture to another. Further, they are related to the projectors P_i for $i = 0, 1, 2$ as

$$\begin{aligned} (\mathbf{1})_{abcd} &= S_{ac}S_{bd} \\ (Q-1)(P_0)_{abcd} &= S_{ab}S_{cd} \\ \text{and } (Q-2)(P_1)_{abcd} &= Q \sum_{\alpha} S_{a\alpha}S_{b\alpha}S_{\alpha c}S_{\alpha d} - S_{ab}S_{cd} . \end{aligned} \quad (3.2.5)$$

Therefore we can write

$$W_{abcd}(f_0, f_1) = (\mathbf{1})_{abcd} + (f_0 + Q^{-1/2}f_1)(Q-1)(P_0)_{abcd} + Q^{-1/2}f_1(Q-2)(P_1)_{abcd} \quad (3.2.6)$$

The weight can also be rewritten in the more physical fashion

$$W_{abcd}(f_0, f_1) = \exp[\mathcal{K}_0(Q-1)P_0 + \mathcal{K}_1(Q-2)P_1] \quad (3.2.7)$$

with

$$\begin{aligned} \exp(\mathcal{K}_0(Q-1)) - 1 &= (f_0 + Q^{-1/2}f_1)(Q-1) , \\ \exp(\mathcal{K}_1(Q-2)) - 1 &= Q^{-1/2}f_1(Q-2) . \end{aligned} \quad (3.2.8)$$

This shows that the Potts model we have built is physical for

$$\begin{aligned} (f_0 + Q^{-1/2}f_1)(Q-1) &> -1 \\ \text{and } Q^{-1/2}f_1(Q-2) &> -1 , \end{aligned}$$

so in particular for $f_0, f_1 > 0$ and $Q > 2$. It presents a mixture of ferromagnetic and antiferromagnetic interactions that will lead to multicritical behaviors (see section 5). It is also interesting to express W in terms of Kronecker delta only. It reads

$$\begin{aligned} W_{abcd}(f_0, f_1) &= \frac{1 - 3Q^{-1/2}f_1 + f_0}{Q^2} + \frac{Q^{-1/2}f_1 - f_0}{Q} (\delta_{ab} + \delta_{cd}) + \frac{Q^{-1/2}f_1 - 1}{Q} (\delta_{ac} + \delta_{bd}) \\ &+ \frac{Q^{-1/2}f_1}{Q} (\delta_{ad} + \delta_{bc}) - Q^{-1/2}f_1 (\delta_{abc} + \delta_{bcd} + \delta_{abd} + \delta_{acd}) \\ &+ \delta_{ac}\delta_{bd} + f_0\delta_{ab}\delta_{cd} + Q^{1/2}f_1\delta_{abcd} \end{aligned} \quad (3.2.9)$$

where

$$\delta_{a_1 \dots a_n} = \begin{cases} 1 & \text{if } a_1 = a_2 = \dots = a_n, \\ 0 & \text{otherwise.} \end{cases}$$

The procedure of writing (3.2.1) in terms of Potts model variables is depicted in fig.(4a) which shows that the local interaction $W_{abcd}(f_0, f_1)$ in (3.2.9) corresponds to the fundamental block \mathcal{G}_2 which is a square with $a b c d$ located at the four corners. Note that the interaction between the four sites are rather complicated as given in (3.2.9).

On the other hand, working with convention B, we have the Potts model weight

$$W'_{abcd}(u) = \sum_{\alpha} S'_{ab} S'_{bd} \left(Q^{-1/2} x_1 + \delta_{b\alpha} \right) \left(1 + Q^{1/2} x_2 \delta_{\alpha d} \right) \left(1 + Q^{1/2} x_3 \delta_{\alpha a} \right) \left(Q^{-1/2} x_4 + \delta_{\alpha c} \right) S'_{ac} S'_{dc} \quad (3.2.10)$$

where

$$S'_{ab} = 1 - \delta_{ab}$$

is the q -symmetrizer, which in this representation simply constrains neighboring sites to have different colors, in which case, it has value one. The weight can likewise be written in terms of projectors as (3.2.6) but with the projectors now given by

$$\begin{aligned} (\mathbf{1})_{abcd} &= \delta_{ad} \mathcal{S}' \\ (Q-1)(P_0)_{abcd} &= \mathcal{S}' \\ (Q-2)(P_1)_{abcd} &= (1 - \delta_{bc}) \mathcal{S}' \end{aligned} \quad (3.2.11)$$

where

$$\mathcal{S}' = S'_{ab} S'_{ac} S'_{bd} S'_{cd}$$

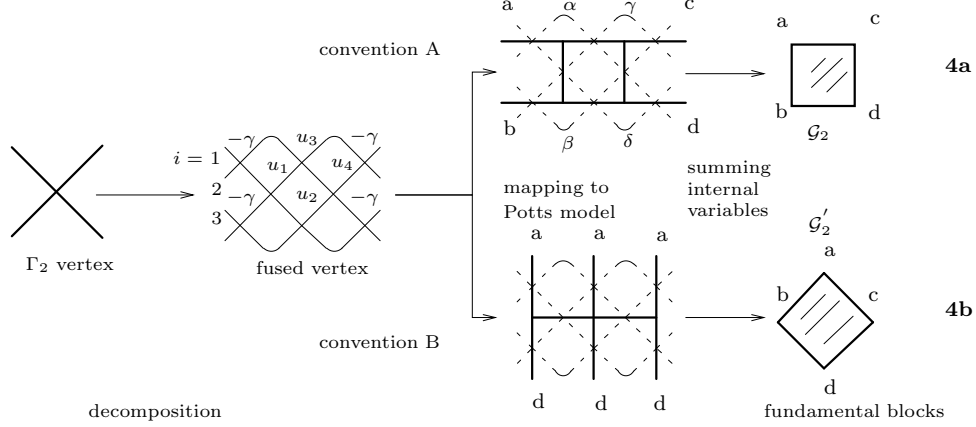
It is then instructive to factor out \mathcal{S}' in the weight leaving

$$W'_{abcd}(f_0, f_1) = \mathcal{S}' (Q^{-1/2} f_1 + \delta_{ad} + f_0 \delta_{bc}), \quad (3.2.12)$$

this is in fact the Potts model considered in [4]. In this form the roles of f_1 and f_0 are more transparent; f_0 can be perceived as the parameter which controls the anisotropy while f_1 controls the four sites interaction induced by the constraint \mathcal{S}' . This constraint imposed by the symmetrizers on the sites is however nontrivial as can be seen in the expansion

$$\begin{aligned} W'_{abcd}(f_0, f_1) &= Q^{-1/2} f_1 - Q^{-1/2} f_1 (\delta_{ab} + \delta_{cd} + \delta_{ac} + \delta_{bd}) + \delta_{ad} + f_0 \delta_{bc} \\ &+ \left(Q^{-1/2} f_1 - f_0 \right) (\delta_{abc} + \delta_{bcd}) + \left(Q^{-1/2} f_1 - 1 \right) (\delta_{abd} + \delta_{acd}) \\ &+ Q^{-1/2} f_1 (\delta_{ac} \delta_{bd} + \delta_{ab} \delta_{cd}) + \left(f_0 - 3Q^{-1/2} f_1 + 1 \right) \delta_{abcd}. \end{aligned} \quad (3.2.13)$$

The mapping to Potts model using convention B is also shown in fig.(4b). The weight (3.2.10) corresponds in the figure to a collection of vertical and horizontal links. Notice that the lattice sites on the top (respectively bottom) rows are identified since they have no Γ_1 vertex between them, and therefore carry the same color a (or d). This gives rise to the 45° rotated square on the rhs of fig (4b.). This rotated square with the variable α summed over is the fundamental block \mathcal{G}'_2 and corresponds to the weight (3.2.13).



Figure(4) The construction of the fundamental blocks $\mathcal{G}_2^{(\prime)}$; Γ_2 vertex is first decomposed into Γ_1 vertices which occupy row $i = 1, 2$ and 3 , the variables $-\gamma, u_1, \dots$ shown next to the vertices are parameters that occur in (3.2.1). When convention A (B) is used, vertices on row $i = 1, 3$ are mapped to horizontal (vertical) links, and that on row $i = 2$ are mapped to vertical (horizontal) links. These two sets of links give rise to the fundamental blocks upon summing the internal sites variables labelled by α, β, \dots .

The above discussion shows that the Potts model representation for the Γ_2 vertex model is achieved by replacing the spin-1 vertex either by \mathcal{G}_2 that corresponds to (3.2.9) or \mathcal{G}_2' that corresponds to (3.2.13). This is an extension of the spin-1/2 case where the Γ_1 vertex is replaced by a horizontal \mathcal{G}_1 or vertical \mathcal{G}_1' link.

For $k = 3$ the vertex is

$$S_3 S_3 r_3(u_1) r_4(u_2) r_5(u_3) r_2(u_4) r_3(u_5) r_4(u_6) r_1(u_7) r_2(u_8) r_3(u_9) S_3 S_3 \quad (3.2.14)$$

with the symmetrizer S_3 given by

$$\begin{aligned} S_3 &= r_1(-\gamma) r_2(-2\gamma) r_1(-\gamma) \\ \tilde{S}_3 &= r_5(-\gamma) r_4(-2\gamma) r_5(-\gamma) . \end{aligned} \quad (3.2.15)$$

The corresponding Potts model Boltzmann weight obtained by convention A has expression

$$W(u)_{aebcfd} = \sum_{\alpha, \beta, \gamma, \delta} S_{ae\alpha} S_{be\beta} \left(\delta_{\alpha\gamma} \delta_{ef} \delta_{\beta\delta} + Q^{-1/2} f_0 \delta_{\alpha\beta} \delta_{\gamma\delta} + f_1 \delta_{\alpha\beta\gamma\delta} + Q^{-1/2} f_2 \delta_{\alpha\gamma} \delta_{\beta\delta} \right) S_{\gamma fc} S_{\delta fd} \quad (3.2.16)$$

where

$$S_{abc} = -\frac{1}{Q-1} (1 - \delta_{ab} - \delta_{bc} - (Q-1)\delta_{ac} + Q\delta_{abc})$$

is the contribution from the symmetrizer and

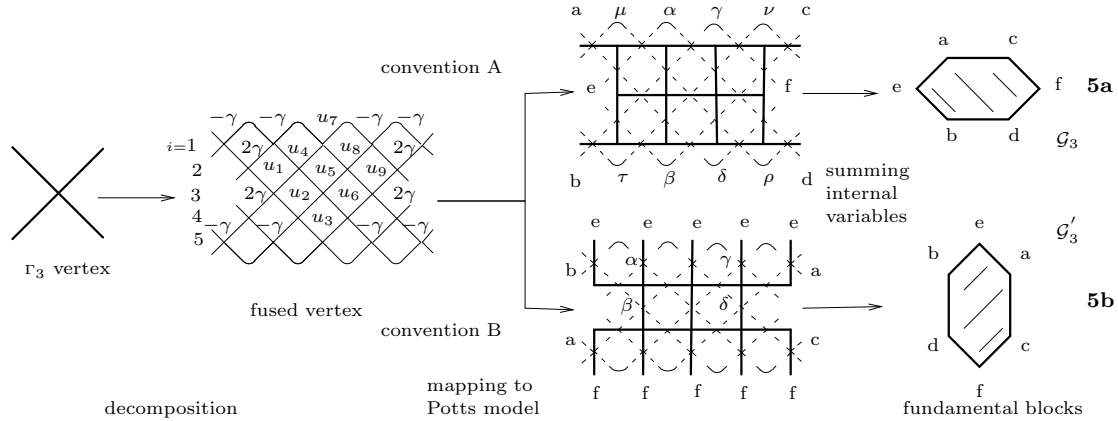
$$\begin{aligned} f_0 &= \prod_{i=1}^9 x_i \\ f_1 &= x_1 x_2 x_4 [x_5 + x_9 + x_5 x_9 (Q^{1/2} + x_6 + x_8) + x_8 x_9 (Q^{1/2} + x_7) + x_6 x_9 (Q^{1/2} + x_3)] \\ &\quad + [x_1 + x_5 + x_1 x_5 (Q^{1/2} + x_2 + x_4) + x_1 x_4 (Q^{1/2} + x_7) + x_1 x_2 (Q^{1/2} + x_3)] x_6 x_8 x_9 \\ &\quad + x_1 x_2 x_4 [(Q^{1/2} + x_5) (Q^{1/2} + x_3 + x_7) + x_3 x_7] x_6 x_8 x_9 + x_1 x_9 (x_2 x_8 + x_4 x_6) \\ f_2 &= x_1 + x_9 + x_1 x_9 [Q^{1/2} + x_4 + x_8 + x_4 x_8 (Q^{1/2} + x_7) + x_2 + x_6 + x_2 x_6 (Q^{1/2} + x_3)] \\ &\quad + x_5 [1 + x_1 (Q^{1/2} + x_2 + x_4)] [1 + x_9 (Q^{1/2} + x_6 + x_8)] \end{aligned} \quad (3.2.17)$$

with x_i 's defined similarly as those in the $k = 2$ case. The four terms in (3.2.16) are again associated to the strand configurations in the geometrical interpretation of the Γ_3 vertex model as shown in fig.(B2). The weight has complicated dependence on a, b, \dots, f , it involves all possible interactions among the six sites. The explicit expression is given in appendix A. The construction is illustrated in fig.(5a). The top two figures on the rhs show that when the variables labelled by Greek letters are summed over, the resulting figure is \mathcal{G}_3 , a hexagonal plaquette with $a \dots d$ occupying the six corners. It corresponds to the weight W_{aebcfd} which depends only on the variables $a \dots d$.

Alternatively, one could map the Γ_3 vertex to the Potts model using convention B. This gives the Boltzmann weight

$$W'(\tilde{u})_{aebcfd} = \sum_{\alpha, \beta, \gamma, \delta} S_{be\alpha} S_{df\beta} (\delta_{\alpha\gamma} \delta_{\beta\delta} + \tilde{f}_0 Q^{1/2} \delta_{\alpha\beta} \delta_{\gamma\delta} \delta_{ef} + \tilde{f}_1 \delta_{\alpha\beta} \delta_{\gamma\delta} + \tilde{f}_2 Q^{1/2} \delta_{\alpha\gamma} \delta_{\beta\delta}) S_{\gamma ea} S_{\delta fc} \quad (3.2.18)$$

where \tilde{f}_0, \tilde{f}_1 and \tilde{f}_2 are similarly defined in terms of \tilde{u}_i as in (3.2.17), and they are decorated with tilde for reason that will be clear in the next few subsections. Graphically, the Potts model weight (3.2.18) corresponds to a hexagon \mathcal{G}'_3 which differ from \mathcal{G}_3 by 90° rotation as shown in the rhs of fig.(5b). Note that in this case, we have also considered the five sites e (f) on the top (bottom) row as a single site for the same reason as in the \mathcal{G}'_2 case.



Figure(5) The construction of the fundamental blocks $\mathcal{G}_3^{(\prime)}$. The procedure is identical to the Γ_2 case, the Γ_1 vertices occupy row $i = 1, \dots, 5$, and contain more parameters $-\gamma, u_1, \dots, u_9$. The two conventions give rise to the fundamental blocks having the same geometrical shape but differ in orientation.

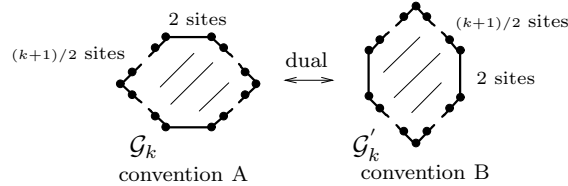
Hitherto, we have demonstrated the construction of the Potts model for $k = 1$ (section 2), 2 and 3. Unlike the $k = 1$ case where the Γ_1 vertex is mapped to a Potts model link (horizontal or vertical), the Γ_2 and Γ_3 vertices are mapped to a set of horizontal and vertical links. These Potts models still reside on square lattices and have inhomogeneous nearest neighbor interaction such as that given in (3.2.2). For the Boltzmann weight, however, it is more natural to sum over the variables associated with the internal sites, such as that labelled by Greek letters in (3.2.2) or fig.(5a) and work with less number of variables which are associated with the sites on the boundary of the fundamental block. In this case, the interactions are no longer restricted to nearest neighbors as can be seen, for example, in (3.2.9). The corresponding

fundamental blocks which depend on less Potts variables are more appropriately regarded as the plaquettes shown in the rhs of figs.(4a),(4b),(5a) and (5b).

These three members of the family of Potts models appear to be quite different from one another, nevertheless we will show they have common symmetry properties . For arbitrary k the Boltzmann weight can in principle be written down following the procedure outlined for $k = 2$ and 3. It is expected to be quite complicated. It depends on k parameters and can be regarded as an operator that acts on k (convention A) or $k + 1$ (convention B) Potts variables. In what follows, we shall mainly discuss the geometrical shape of the fundamental block \mathcal{G}_k (\mathcal{G}'_k) for arbitrary k .

For k odd, the Γ_k vertex maps either to a hexagonal plaquette \mathcal{G}_k with four slanted edges and two horizontal edges by convention A or to a hexagonal plaquette \mathcal{G}'_k that has four slanted edges and two vertical edges by convention B. The number of lattice sites on each slanted edge is equal to $(k + 1)/2$, while there are two sites on the horizontal and vertical edges (see fig.(6)). The case of $k = 1$ is a degenerate situation where the slanted edge shrinks to a lattice site and the hexagon is flattened to become a vertical or horizontal link.

It is not difficult to arrive at the shape of the fundamental block. In the Potts model language, the symmetrizer S_k , which consists of the vertices r_i, \dots, r_{i+k-1} involves $(k + 1)/2$ sites since k is odd. These Potts sites are those residing on the slanted edge. The top and bottom rows of Γ_1 vertices have odd subscripts. When convention A is used, they are mapped to horizontal links which becomes the two horizontal edges of the hexagon. There are $2k$ Potts sites on each of these horizontal edge, but $2k - 2$ of them are internal. As an example for $k = 3$ (see fig.(5a)), the four Greek letters label the internal sites. When the variables associated with these internal sites are summed over in the Boltzmann weight, the horizontal edge effectively carries two sites. In the $k = 3$ case, they are labelled by $a c$ and $b d$. When convention B is used, the top and bottom rows of Γ_1 vertices are mapped to vertical links. The lattice sites on the top and bottom rows are respectively identified due to the fact that there are no Γ_1 vertices between them (see for example fig.(5b)). The Γ_1 vertices which are midway from the top and bottom rows are mapped to vertical edges, which eventually form the vertical edges of the hexagon \mathcal{G}'_k .

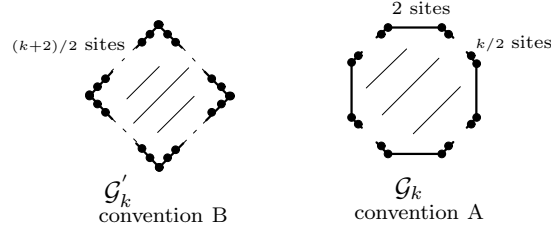


Figure(6) The fundamental blocks obtained by convention A and B for odd k model

For k even, the fundamental block \mathcal{G}_k obtained using convention A is an octagon with two vertical and horizontal edges each carrying two Potts sites, and four slanted edges with $k/2$ Potts sites on each of them (see fig.(7)). For $k = 2$, the slanted edge reduces to a single Potts site and the octagon becomes a square. When convention B is used, the fundamental block \mathcal{G}'_k is a 45° rotated square with $k/2$ sites on every edge.

In both conventions, the slanted edges are originated from the symmetrizers S_k , which acts on $(k + 2)/2$ or $k/2$ lattice sites since k is even. For convention A, vertices at the top and bottom rows are associated with vertical edges, while vertices midway from the top and bottom rows are associated with horizontal edges, these edges are the two vertical and horizontal ones of the octagon. For convention B, all Potts sites on the top and bottom rows are respectively identified for the same reason given in the odd k case, they therefore become the top and bottom corners of the 45° rotated square. The other two corners of the

rotated square come from vertices midway from the top and bottom rows, which are associated with horizontal edges. Finally in arriving at the shape of the fundamental blocks, we have assumed that internal sites variables are summed over.

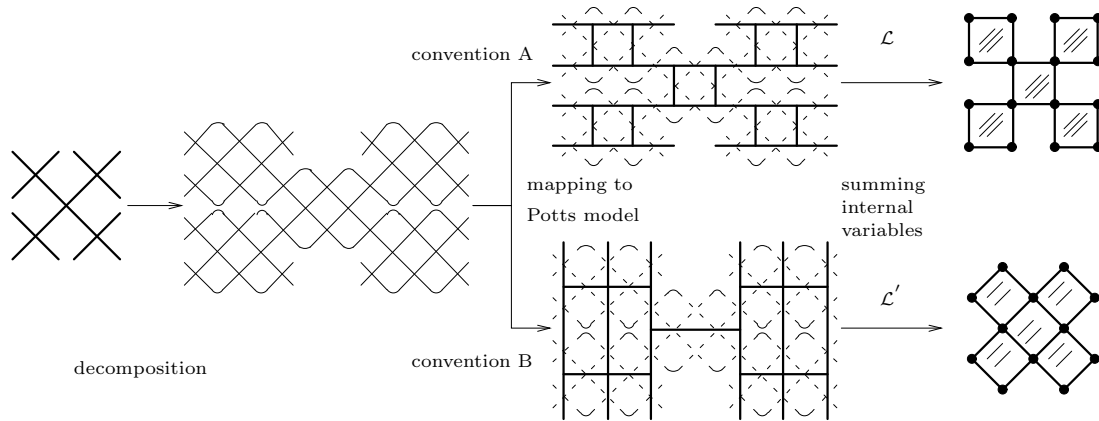


Figure(7) The fundamental blocks obtained by convention A and B for even k model

3.3 The patching

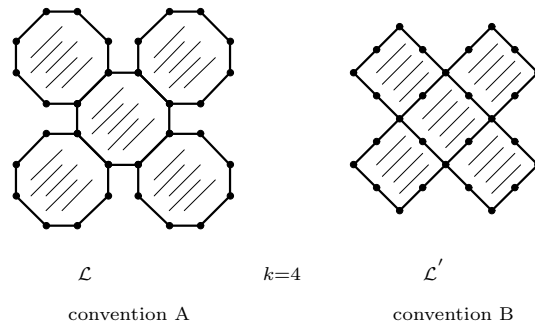
The previous subsection deals with the construction of the local weight $W^{(\prime)}$ of the Potts model and also the fundamental block $\mathcal{G}_k^{(\prime)}$. These fundamental blocks are the building block of the lattice just as in the Γ_1 Potts model the lattice is constructed from vertical and horizontal links, which, in our notation, are \mathcal{G}_1 and \mathcal{G}'_1 . Since there are two conventions (A or B) to be used in getting the Potts model, two lattices can be constructed. They are denoted as \mathcal{L} and \mathcal{L}' . Detailed analysis shows a splitting between k even and k odd cass.

For k even, we use the Γ_2 vertex model as an example. Beginning with the vertex model lattice, we replace each of the Γ_2 vertices by the fundamental block. For convention A, this gives rise to a Potts model lattice \mathcal{L} which resembles a square check board [19]. First, each Γ_2 vertex is replaced by the fused vertex (3.2.1) shown in fig.(2), and subsequently this fused vertex is mapped using convention A to the square \mathcal{G}_2 which has only lattice sites on the four corners. Neighboring \mathcal{G}_2 's are connected along the NE-SW or NW-SE direction by sharing a lattice site on their common corner. For convention B, the lattice \mathcal{L}' is a 45° rotated square lattice. This is obtained by replacing each fused vertex with the 45° rotated square plaquette \mathcal{G}'_2 and glueing neighboring \mathcal{G}'_2 along the slanted edge. In this case, \mathcal{L} and \mathcal{L}' are both square lattices, however, the former is check board like and only alternate squares are given Boltzmann weight W , while the later has all squares associated with the weight W' . See fig.(8) for the construction of the two lattices.



Figure(8) Construction of the Γ_2 Potts model lattices where the procedure is illustrated using five neighboring Γ_2 vertices.

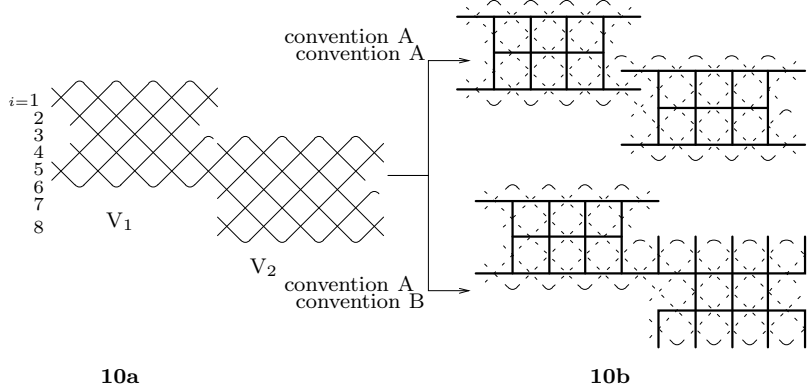
It is straight forward to extend the above to arbitrary even k . For convention A, we replace each of the Γ_k vertices by the octagon \mathcal{G}_k , and neighboring octagons are connected along the NE-SW or NW-SE direction by glueing together pairs of slanted edges. The resulting lattice \mathcal{L} is shown in fig.(9a) (for $k = 4$) where the filled circles denote the lattice sites. For convention B, the Γ_k vertices are mapped to 45° rotated square plaquettes \mathcal{G}'_k , the resulting lattice \mathcal{L}' is a 45° rotated square lattice just like the $k = 2$ lattice \mathcal{L}' , however, there are $(k + 2)/2$ lattice sites on every edge (see fig.(9b) for $k = 4$).



Figure(9a) The Γ_4 Potts model lattice from convention A

Figure(9b) The Γ_4 Potts model lattice from convention B

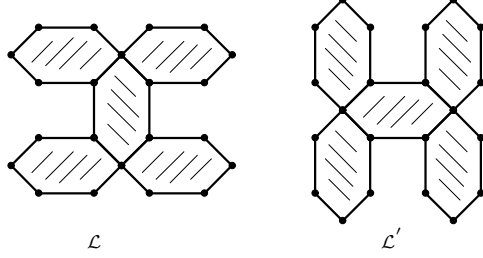
For k odd, we use the Γ_3 model as an example. Recall that \mathcal{G}_3 and \mathcal{G}'_3 differ by 90° rotation, we expect therefore the lattices \mathcal{L} and \mathcal{L}' to have similar symmetry properties.



Figure(10) The two possible patching of the fundamental blocks from the neighboring vertices V_1 and V_2 . The top figure on the rhs uses convention A for the neighboring Γ_3 vertices, the resulting Potts lattices are not compatible. The bottom figure shows the correct mapping where different conventions are used on neighboring Γ_3 vertices.

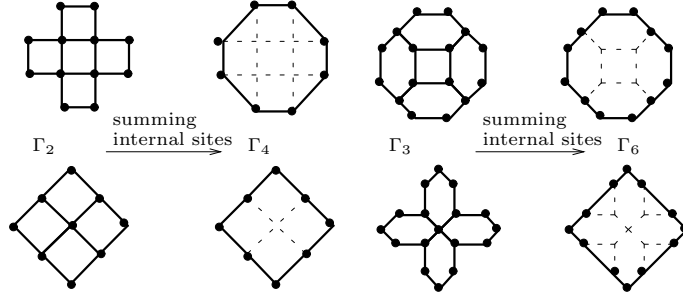
As before we first replace each Γ_3 vertex by the fused vertex (3.2.1) shown in fig.(2) and consider two neighboring fused vertices connected along the NW-SE direction. Let us denote them as V_1 and V_2 respectively (see fig.(10a)) where V_1 is on the upper left corner of V_2 . The Γ_1 vertices that belong to V_1 are r_1, \dots, r_5 and that belong to V_2 are r_4, \dots, r_8 . The symmetrizers S_3 's that connect V_1 and V_2 occupy rows $i = 4$ and 5 , ie. they are made out of r_4 and r_5 . Suppose V_1 is mapped to the Potts model fundamental block \mathcal{G}_3 using convention A, the Γ_1 vertices r_4 and r_5 will be mapped respectively to a vertical and a horizontal link. However, this implies that the Γ_1 vertices on the top row of V_2 , which are r_4 , have to be mapped accordingly to vertical links so that the two set of Potts model links obtained from V_1 and V_2 are compatible. In other words, convention B has to be used on V_2 which replaces V_2 by \mathcal{G}'_3 . This point is illustrated in fig.(10b).

Hence, neighboring Γ_3 vertices are to be mapped to Potts model links using different conventions. The resulting lattice \mathcal{L} has the geometry shown in the lhs of fig.(11). If the mapping of V_1 is done with convention B, the lattice \mathcal{L}' obtained (see rhs of fig.(11)) is related to \mathcal{L} by replacing all \mathcal{G}_3 by \mathcal{G}'_3 and vice versa. This feature is present in all odd k models. For the Γ_1 Potts model, vertical \mathcal{G}'_1 and horizontal \mathcal{G}_1 links are associated respectively to neighboring vertices connected along the NE-SW or NW-SE direction. For higher odd k , the Potts model lattice \mathcal{L} or \mathcal{L}' have to be constructed with both \mathcal{G}_k and \mathcal{G}'_k , for the same reason as in the $k = 3$ case, ie. the symmetrizer S_k contains even number of rows of Γ_1 vertices. Since $\mathcal{G}_k^{(i)}$ has the same hexagonal shape for $k \geq 3$, the lattice \mathcal{L} and \mathcal{L}' are identical to that of the $k = 3$ model except that there are $(k + 1)/2$ lattices on the slanted edge.



Figure(11) The Γ_3 Potts model lattices

Graphically, it is easy to see that four neighboring blocks $\mathcal{G}_k^{(\prime)}$ of the Γ_k Potts model can be combined in a natural way to form the fundamental block \mathcal{G}_{2k} or \mathcal{G}'_{2k} of the Γ_{2k} Potts model (see fig.(12)). Nonetheless, this does not imply that a Γ_k Potts model can also be considered, after summation over the appropriate variables, as Γ_{2k} Potts model. Although the geometry is the same, the full definition of the Γ_k Potts models implies that they are built from a vertex model with spin $k/2$ representation of $U_q\text{su}(2)$, and this constrains the form of the Boltzmann weights. Figure (12) looks like one step in real space renormalization group. The fact that starting from a Γ_k Potts model one does not get a Γ_{2k} suggests that the Γ_k Potts models for different values of k belong a priori to different universality classes.



Figure(12) Relation between \mathcal{G}_k and \mathcal{G}_{2k} . The cases of $k = 2, 3$ are illustrated which shows that four neighboring \mathcal{G}_k have the geometry of a \mathcal{G}_{2k} .

3.4 Isotropy of the Potts model

We consider now some symmetries of these Potts models. First, it is clear that for arbitrary k the weight W is invariant under reflection of the the fundamental block about a horizontal or vertical line drawn across its center. As an example, the weight W of the $k = 2$ model is invariant under the following reflections;

$$\begin{array}{l}
 \text{reflection about vertical line} \\
 \text{reflection about horizontal line}
 \end{array}
 \left\{ \begin{array}{ll}
 (a b c d) \longrightarrow (c d a b) & \mathcal{G}_2, \\
 (a b c d) \longrightarrow (a c b d) & \mathcal{G}'_2, \\
 (a b c d) \longrightarrow (b a d c) & \mathcal{G}_2, \\
 (a b c d) \longrightarrow (d b c a) & \mathcal{G}'_2,
 \end{array} \right. \quad (3.4.1)$$

where a, \dots, d are Potts model variables associated to the lattice sites on the boundary of \mathcal{G}_2 and \mathcal{G}'_2 as given in figs.(4a) and (4b).

In addition, for k even, the fundamental block has 90° rotational symmetry about its center. The weight associated to the fundamental block however does not remain unchanged under such a rotation. We first consider the $k = 2$ model. The 90° rotation is given, using the notation of figs.(4a) and (4b), by

$$(a b c d) \longrightarrow (c a d b) \quad (3.4.2)$$

for both \mathcal{G}_2 and \mathcal{G}'_2 . Under rotation, the corresponding weights undergo the transformation;

$$\begin{aligned} W(f_0, f_1) &\longrightarrow f_0 W_{90^\circ}(f_0^{-1}, f_0^{-1} f_1), \\ W'(f_0, f_1) &\longrightarrow f_0 W'_{90^\circ}(f_0^{-1}, f_0^{-1} f_1), \end{aligned} \quad (3.4.3)$$

and for $f_0 = 1$ they are invariant. We shall refer to this symmetry as **face isotropy**. Face isotropy is also present in higher even k models. To examine the behavior of the weight under this rotation, we recall that the underlying Γ_k vertex has k independent parameters which can be taken as the coefficients of the projectors P_j ; $j = 1, \dots, k$. However, a more convenient choice for our purpose is provided by the weights of the $k + 1$ strand configurations from the loop model realization of the Γ_k vertex model as explained in appendix B. This set of configurations for k even contains a special element which is invariant under 90° rotation (for the case of $k = 2$, it is given by the last picture in fig.(B1)). The others group naturally into $k/2$ pairs such that configurations that belong to the same pair differ only by 90° rotation (again, if we refer to fig.(B1), the first and second pictures belong to the same pair). The parameters of the Boltzmann weight of the Γ_k Potts model can now be taken as the weights of these strand configurations. They are denoted as $(f_0, 1), (f_1, f_{k-1}), \dots, (f_{(k-2)/2}, f_{(k+2)/2})$ and $f_{k/2}$ where the brackets enclose the weights of the paired up configurations. Rotation of \mathcal{G}_k or \mathcal{G}'_k about its center corresponds to rotation of the strands configuration and is thus given by the following transformation of the parameters;

$$\begin{aligned} f_0 &\longrightarrow f_0^{-1}, \\ f_i f_0^{-1/2} &\longrightarrow f_{k-i} f_0^{-1/2} \quad ; i = 1, \dots, k-1, \end{aligned} \quad (3.4.4)$$

which is obtained by rescaling the weight $W^{(\prime)}$ by f_0 and using the fact that configurations that belong to the same pair are interchanged by the 90° rotation. From the above it is clear that face isotropy is achieved when

$$\begin{aligned} f_0 &= 1, \\ f_i &= f_{k-i} \quad ; i = 1, \dots, (k-2)/2, \end{aligned} \quad (3.4.5)$$

which reduces the number of parameters to $k/2$.

For k odd, there is no face isotropy since the hexagonal fundamental blocks are not invariant under 90° rotation.

Next, we examine the behavior of the Potts model under 90° rotation of the lattice and shall refer to such a symmetry as **lattice isotropy**. We shall study the **staggered** case where weights of \mathcal{G}_k that are neighboring to each other have independent sets of parameters, so the model depends on $2k$ parameters (in the following, staggered and homogeneous refer implicitly to the underlying vertex model). Lattice isotropy can then exist in both even and odd k models. In fact, eventhough the lattice structures are very different between the odd and even k models as pointed out earlier, their parameters basically behave the same under

rotation of lattice. As an example, we first consider the staggered Γ_3 Potts model. Recall that the lattice is constructed out of \mathcal{G}_3 and \mathcal{G}'_3 , and since the model is staggered, the two sets of parameters f_0, f_1, f_2 and $\tilde{f}_0, \tilde{f}_1, \tilde{f}_2$ that belong respectively to the weights (3.2.16), (3.2.18) of \mathcal{G}_3 's and \mathcal{G}'_3 's are considered to be independent. To examine the transformation of the weights, we first rewrite them as

$$\begin{aligned} W'(\tilde{f}_0, \tilde{f}_1, \tilde{f}_2)_{aebcfd} &= Q^{1/2} \tilde{f}_0 \sum_{\alpha, \beta, \gamma, \delta} S_{be\alpha} S_{df\beta} (\delta_{\alpha\beta} \delta_{\gamma\delta} \delta_{ef} + Q^{-1/2} \tilde{f}_0^{-1} \delta_{\alpha\gamma} \delta_{\beta\delta} + \tilde{f}_2 \tilde{f}_0^{-1} \delta_{\alpha\gamma} \delta_{\beta\delta}) \\ &\quad + Q^{-1/2} \tilde{f}_1 \tilde{f}_0^{-1} \delta_{\alpha\beta} \delta_{\gamma\delta} S_{\gamma ea} S_{\delta fc}, \\ W(f_0, f_1, f_2)_{aebcfd} &= Q^{-1/2} f_0 \sum_{\alpha, \beta, \gamma, \delta} S_{ae\alpha} S_{be\beta} (\delta_{\alpha\beta} \delta_{\gamma\delta} + f_0^{-1} Q^{1/2} \delta_{\alpha\gamma} \delta_{ef} \delta_{\beta\delta} + f_2 f_0^{-1} \delta_{\alpha\gamma} \delta_{\beta\delta}) \\ &\quad + f_1 f_0^{-1} Q^{1/2} \delta_{\alpha\beta\gamma\delta} S_{\gamma fc} S_{\delta fd}. \end{aligned} \quad (3.4.6)$$

$$(3.4.7)$$

After the rotation of the lattice, (3.4.6) and (3.4.7) correspond to weights of \mathcal{G}_3 and \mathcal{G}'_3 respectively, we therefore compare (3.4.6) with (3.2.16) and (3.4.7) with (3.2.18). This implies the following relation between the partition functions before and after the rotation

$$Z(f_0, f_1, f_2; \tilde{f}_0, \tilde{f}_1, \tilde{f}_2) = (f_0 \tilde{f}_0)^N Z_{90^\circ}(\tilde{f}_0^{-1}, \tilde{f}_2 \tilde{f}_0^{-1}, \tilde{f}_1 \tilde{f}_0^{-1}; f_0^{-1}, f_2 f_0^{-1}, f_1 f_0^{-1}), \quad (3.4.8)$$

where N denotes the total number of underlying Γ_3 vertices of the model. Clearly, lattice isotropy is given by

$$\begin{aligned} f_0 &= \tilde{f}_0^{-1}, \\ f_1 f_0^{-1/2} &= \tilde{f}_2 \tilde{f}_0^{-1/2}, \\ f_2 f_0^{-1/2} &= \tilde{f}_1 \tilde{f}_0^{-1/2}. \end{aligned} \quad (3.4.9)$$

It is straight forward to extend the study of the lattice symmetry to higher k models. For k odd, we again adopt the parametrization offered by the weights of the strand configurations. However, there are now two sets of identical strands configurations from neighboring \mathcal{G}_k and \mathcal{G}'_k , the parameters are $(f_0, 1), (f_1, f_{k-1}), \dots, (f_{(k-1)/2}, f_{(k+1)/2})$ and $(\tilde{f}_0, 1), (\tilde{f}_1, \tilde{f}_{k-1}), \dots, (\tilde{f}_{(k-1)/2}, \tilde{f}_{(k+1)/2})$ where the first and second sets belong respectively to the weights of \mathcal{G}_k and \mathcal{G}'_k . Parameters are paired up according to the same criterion as before. Notice that in this case there is no strand configuration which is invariant under 90° rotation. For the $k = 3$, these are precisely the parameters that appear in (3.2.16) and (3.2.18). Since rotation of the lattice by 90° turns \mathcal{G}_k into \mathcal{G}'_k and vice versa, and also interchanges configurations that belong to the same pair, we have the following mapping of the parameters

$$\begin{aligned} f_0 &\longleftrightarrow \tilde{f}_0^{-1}, \\ f_i f_0^{-1/2} &\longleftrightarrow \tilde{f}_{k-i} \tilde{f}_0^{-1/2} \quad ; i = 1, \dots, k-1. \end{aligned} \quad (3.4.10)$$

Thus, the model with lattice isotropy has k parameters where

$$\begin{aligned} f_0 &= \tilde{f}_0^{-1}, \\ f_i f_0^{-1/2} &= \tilde{f}_{k-i} \tilde{f}_0^{-1/2} \quad ; i = 1, \dots, k-1. \end{aligned} \quad (3.4.11)$$

For even k , similar situation occurs. We again use the weights of the strand configurations as parameters, which read $(f_0, 1), (f_1, f_{k-1}), \dots, (f_{(k-2)/2}, f_{(k+2)/2}), f_{k/2}$ and $(\tilde{f}_0, 1), (\tilde{f}_1, \tilde{f}_{k-1}), \dots, (\tilde{f}_{(k-2)/2}, \tilde{f}_{(k+2)/2}), \tilde{f}_{k/2}$.

These two sets of parameters again correspond respectively to the weights of neighboring \mathcal{G}_k 's. The only difference between this model and the previous one is that the entire lattice is constructed out of \mathcal{G}_k or \mathcal{G}'_k exclusively. Under 90° rotation of the lattice, the parameters transform as

$$\begin{aligned} f_0 &\longleftrightarrow \tilde{f}_0^{-1}, \\ f_i f_0^{-1/2} &\longleftrightarrow \tilde{f}_{k-i} \tilde{f}_0^{-1/2} \quad ; i = 1, \dots, k-1, \end{aligned} \quad (3.4.12)$$

for similar reasons as in the odd k case. The Potts model with lattice isotropy is given by

$$\begin{aligned} f_0 &= \tilde{f}_0^{-1}, \\ f_i f_0^{-1/2} &= \tilde{f}_{k-i} \tilde{f}_0^{-1/2} \quad ; i = 1, \dots, k-1, \end{aligned} \quad (3.4.13)$$

and has k independent parameters.

Conditions (3.4.11) and (3.4.13) both define staggered models in general.

The above transformations of the parameters show conversely that the **homogeneous** model where

$$\begin{aligned} f_0 &= \tilde{f}_0, \\ f_i &= \tilde{f}_i \quad ; i = 1, \dots, k-1, \end{aligned} \quad (3.4.14)$$

is in general not invariant under the rotation of the lattice except when face isotropy is present in every \mathcal{G}_k 's weight and this applies only to even k models.

3.5 Self duality

In the construction of the Γ_k Potts model, there exist two possible conventions (A or B) that can be used. These two choices give rise to two lattices. For k odd, the lattices \mathcal{L} and \mathcal{L}' have identical structure due to the fact that both \mathcal{G}_k and \mathcal{G}'_k have to be used, while for even k , \mathcal{L} and \mathcal{L}' are different. Let us discuss the relation between the models obtained by conventions A and B in more details. We consider a general staggered Potts model. We first look at the Γ_1 Potts model to examine the origin of this two choices. We have, in the notation of this section, neighboring Γ_1 vertices X_{2i-1} and X_{2i} given by

$$\begin{aligned} X_{2i-1} &= \mathbf{1} + f_0 e_{2i-1}, \\ X_{2i} &= \mathbf{1} + \tilde{f}_0 e_{2i} \end{aligned} \quad (3.5.1)$$

where f_0 and \tilde{f}_0 are independent (they should be identified with x_1^{-1}, x_2 defined in section 2). Mapping to Potts model using convention A, we replace X_{2i-1} and X_{2i} respectively by horizontal and vertical links. The vertices in terms of Potts model variables read

$$\begin{aligned} (X_{2i-1})_{ab} &= \delta_{ab} + f_0 Q^{-1/2}, \\ (X_{2i})_{bc} &= 1 + \tilde{f}_0 Q^{1/2} \delta_{bc}, \end{aligned} \quad (3.5.2)$$

where $a b$ and $b c$ are the sites on the horizontal and vertical links. After duality transformation [1] X_{2i-1} and X_{2i} are instead associated to a vertical and horizontal link, which corresponds to convention B

$$\begin{aligned} (X_{2i-1})_{bc} &= 1 + f_0 Q^{1/2} \delta_{bc}, \\ (X_{2i})_{ab} &= \tilde{f}_0 Q^{-1/2} + \delta_{ab}, \end{aligned} \quad (3.5.3)$$

where we stick to the convention that a b (\bar{b} c) are sites on the horizontal (vertical) link. This implies, following fusion, that for arbitrary k , the Potts models obtained by conventions A and B are related by duality transformation.

Combining the above argument with result of subsection 3.3 on the structure of the lattices \mathcal{L} and \mathcal{L}' , we see that the question of self duality does not arise for the family of even k Potts models since the lattice \mathcal{L} and its dual \mathcal{L}' are not the same. But for k odd, self duality can occur since both \mathcal{L} and \mathcal{L}' have the same structure. The self duality condition can be easily identified for the Γ_1 Potts model by comparing (3.5.2) with (3.5.3). We see that duality transformation amounts to

$$f_0 \longleftrightarrow \tilde{f}_0, \quad (3.5.4)$$

which is equivalent to (2.11). For higher odd k models, similar transformation of the parameters can be deduced by using the fact that duality map is equivalent to interchanging convention A with convention B. Thus using the same set of parameters as in the previous subsection, the duality transformation is given by

$$\begin{aligned} f_0 &\longleftrightarrow \tilde{f}_0, \\ f_i &\longleftrightarrow \tilde{f}_i \quad ; i = 1, \dots, k-1. \end{aligned} \quad (3.5.5)$$

And self duality is given by the condition

$$\begin{aligned} f_0 &= \tilde{f}_0, \\ f_i &= \tilde{f}_i \quad ; i = 1, \dots, k-1. \end{aligned} \quad (3.5.6)$$

which means that the model becomes **homogeneous** with k parameters. If the Γ_k Potts model has lattice isotropy to begin with, then self duality map is given by

$$\begin{aligned} f_0 &\longleftrightarrow f_0^{-1}, \\ f_i f_0^{-1/2} &\longleftrightarrow f_{k-i} f_0^{-1/2} \quad i = 1, \dots, k-1. \end{aligned} \quad (3.5.7)$$

where the relation (3.4.11) has been used. Thus imposing the conditions of self duality and lattice isotropy, the number of parameters reduces to $(k-1)/2$ since we now have

$$\begin{aligned} f_0 &= \tilde{f}_0 = 1 \\ f_i &= f_{k-i} = \tilde{f}_i = \tilde{f}_{k-i} \quad ; i = 1, \dots, (k-1)/2. \end{aligned} \quad (3.5.8)$$

Recall that in the case $k=1$ these conditions determined completely the Potts model interaction.

3.6 Integrability

We conclude this section by discussing some special cases of the Potts models which are known to be integrable. For simplicity, we restrict ourselves to the homogeneous models. In this restricted class, the Γ_1 distinguishes itself from the rest in that it is integrable for any f_0 . The corresponding R matrix can be written as

$$\check{R}(u) = 1 + \frac{\sin u}{\sin(\gamma - u)} e, \quad (3.6.1)$$

where

$$f_0 = \frac{\sin u}{\sin(\gamma - u)} .$$

For higher k , only subsets of the full parameter space are integrable. A standard such case is obtained from the special choice in (3.1.4)

$$\begin{cases} u_j = u_{j+1} - \gamma & ; (i-1)k < j \leq ik < k^2 , \\ u_{ik} = u + (i-1)\gamma & ; i = 1, \dots, k , \end{cases} \quad (3.6.2)$$

where u is the spectral parameter of the R matrix . We shall refer to this as the **JB** integrable line as this is constructed by Jimbo in [5]. The R matrix for this Γ_k model can also be written as a linear combination of projectors;

$$\check{R}(u) = P_{j=k} + \frac{y^2 - q^{2k}}{1 - y^2 q^{2k}} P_{j=k-1} + \dots + \frac{y^2 - q^{2k}}{1 - y^2 q^{2k}} \frac{y^2 - q^{2(k-1)}}{1 - y^2 q^{2(k-1)}} \dots \frac{y^2 - q^2}{1 - y^2 q^2} P_{j=0} , \quad (3.6.3)$$

where $y = \exp(-iu)$ is the multiplicative spectral parameter. The corresponding Potts model is also integrable since the fact that Yang Baxter equation is satisfied is expressed algebraically, without reference to a particular representation. In terms of the parameters f_i 's of the Γ_2 and Γ_3 Potts models the JB integrable line is given by the following formula

$$\begin{cases} \Gamma_2 & \begin{cases} f_0 = \frac{\sin(u) \sin(\gamma + u)}{\sin(2\gamma - u) \sin(\gamma - u)} , \\ f_1 = \frac{Q^{1/2} \sin u}{\sin(2\gamma - u)} , \end{cases} \\ \Gamma_3 & \begin{cases} f_0 = \frac{\sin u \sin(u + \gamma) \sin(u + 2\gamma)}{\sin(\gamma - u) \sin(2\gamma - u) \sin(3\gamma - u)} , \\ f_1 = \frac{(Q-1) \sin u \sin(u + \gamma)}{\sin(3\gamma - u) \sin(2\gamma - u)} , \\ f_2 = \frac{(Q-1) \sin u}{\sin(3\gamma - u)} . \end{cases} \end{cases} \quad (3.6.4)$$

In terms of the spectral parameter u , rotation of the lattice by 90° is given by

$$u \longrightarrow \gamma - u .$$

This transformation of u actually applies to all the Γ_k models on the JB integrable line. The condition for lattice isotropy $f_0 = 1$ is therefore equivalent to $u = \gamma/2$, and the parameters f_i 's read

$$\begin{cases} \Gamma_2 & \begin{cases} f_0 = 1 , \\ f_1 = \frac{Q^{1/2}}{Q^{1/2} + 1} , \end{cases} \\ \Gamma_3 & \begin{cases} f_0 = 1 \\ f_1 = f_2 = \frac{(Q-1)}{Q + Q^{1/2} - 1} . \end{cases} \end{cases} \quad (3.6.5)$$

Besides the JB integrable line there is another integrable line in all Γ_k models, which is related to the Temperley-Lieb algebra. For arbitrary k , since the projector $(k+1)_q P_0$ satisfies the Temperley-Lieb algebra[17] with

$$\begin{aligned} e &= (k+1)_q P_0 \\ \text{and } e^2 &= (k+1)_q e , \end{aligned} \quad (3.6.6)$$

the R matrix

$$\check{R}(u) = \mathbf{1} + \frac{\sin u}{\sin(\gamma - u)}(k + 1)_q P_0 \quad (3.6.7)$$

satisfies the Yang-Baxter equation with u being the spectral parameter. We shall refer to this line as the **TL** integrable line. Obviously, for $k = 1$, the TL and JB lines coincide. The Potts model which corresponds to the above R matrix (3.6.7) has parameters given by

$$\begin{aligned} f_0 &= \frac{\sin u}{\sin(\gamma - u)}, \\ f_i &= 0 \quad ; i = 1, \dots, k - 1. \end{aligned} \quad (3.6.8)$$

For $k \geq 2$, these two lines JB and TL do not exhaust all the integrable cases. As an example, for the Γ_2 model, there is an additional integrable line given by

$$\begin{aligned} f_0 &= -\frac{\sin(u) \cos(\gamma - u)}{\sin(2\gamma - u) \cos(3\gamma - u)}, \\ f_1 &= \frac{Q^{1/2} \sin u}{\sin(2\gamma - u)}, \end{aligned} \quad (3.6.9)$$

which is related to the Izergin-Korepin model[16]. In this case the model with lattice isotropy is given by

$$u = 3\gamma/2 + \pi/4 \quad (3.6.10)$$

or

$$\begin{aligned} f_0 &= 1, \\ f_1 &= -(q + q^{-1})(1 + i(q - q^{-1})). \end{aligned} \quad (3.6.11)$$

4 The Spontaneous Magnetization

4.1 Definitions

The spontaneous magnetization of the usual (Γ_1) Potts model on the first order transition line has been computed exactly by Baxter[20] using the method of corner transfer matrix (CTM). We will show in this section that using the fusion procedure, spontaneous magnetizations of the homogeneous Γ_k Potts model can similarly be computed. As for $k = 1$ the model is expected to undergo a first order phase transition along the JB integrable line for $Q > 4$ [1],[24]. In what follows, we shall restrict Q to this range and replace γ by $-i\lambda$ with λ being real, thus

$$\sqrt{Q} = 2 \cosh \lambda \quad (4.1.1)$$

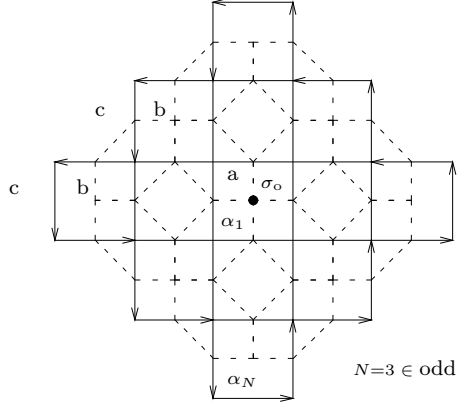
and work exclusively on the JB integrable line.

To define the spontaneous magnetization for the fused Potts model, we generalize the work of [20] and consider some fundamental block \mathcal{G}_k (or \mathcal{G}'_k) sufficiently remote from the boundary and fix a site σ_o which we shall refer to as central site. The spontaneous magnetization is then defined as

$$M = \frac{Q \langle \delta_{\sigma_o, 1} \rangle - 1}{Q - 1} \quad (4.1.2)$$

where

$$\langle \delta_{\sigma_o,1} \rangle = Z_{\text{Potts}}^{-1} \sum_{\{\sigma\}} \delta_{\sigma_o,1} \prod_{\mathcal{G}_k^{(i)}} W(\mathcal{G}_k^{(i)}) .$$



Figure(13) The geometry of the Γ_k Potts model lattice; a, b, c are the face variables, the central site σ_o is taken in the figure to be the filled circle at the center, and the spin variables are denoted by the α_i where $i = 1$ and N are shown.

For the sake of computation, we consider the underlying Γ_k vertex model lattice to be an $l \times l$ square as in fig.(13) where we show the Γ_k (k odd in this case) vertices and the respective fundamental blocks \mathcal{G}_k , the α_i 's denote the spin- $\frac{k}{2}$ arrows which can have $k + 1$ states $\frac{k}{2}, \frac{k}{2} - 1, \dots, -\frac{k}{2}$, and i takes values from 1 to N with N taken to be odd always. As for $k = 1$ the boundary conditions are conveniently defined in terms of the vertex degrees of freedom: we require that the spin arrows along the perimeter all have the same state. This provides $k + 1$ boundary conditions of which we assume (more later) that they select different phases of the Γ_k Potts model.

Recall that each spin- $\frac{k}{2}$ arrow can be regarded from the fusion point of view as being made up of k spin- $\frac{1}{2}$ arrows. These spin- $\frac{1}{2}$ arrows form surrounding polygons for the Potts model links, in particular, due to the boundary condition, the perimeter can be viewed as k polygons enclosing the Potts model. We then define the central site σ_o to be connected to the boundary if there is no spin- $\frac{1}{2}$ surrounding polygon enclosing it other than those from the perimeter. With this definition, we can now relate the spontaneous magnetization to the percolation probability P defined as the probability of σ_o being connected to the boundary. It is easy to see that

$$\langle \delta_{\sigma_o,1} \rangle = Q^{-1}(1 - P) + P \quad (4.1.3)$$

and

$$M = P . \quad (4.1.4)$$

As in the case of Γ_1 Potts model, the percolation probability can be expressed in terms of variables of the vertex model. Referring to fig.(13), we define the following quantity [21]

$$S(\alpha) = e^{-(i\pi+2\lambda)(\alpha_1+\dots+\alpha_{N-1})} \quad (4.1.5)$$

and its expectation value

$$\langle S(\alpha) \rangle = Z_{\text{vertex}}^{-1} \sum_{\{\alpha\}} S(\alpha) \prod (\text{vertex weight}) . \quad (4.1.6)$$

Recall that closed loop formed by the spin- $\frac{1}{2}$ surrounding polygon has orientation given by that of the spin arrow, and it acquires a weight $(e^\lambda) e^{-\lambda}$ when the direction is (anti-)clockwise. Writing the α_i 's in $S(\alpha)$ as sum of spin- $\frac{1}{2}$ states, it is clear that when σ_o is connected to the boundary, there are as many left pointing spin- $\frac{1}{2}$ arrows among $\alpha_1, \dots, \alpha_{N-1}$ as there as right pointing ones, giving

$$S(\alpha) = 1 .$$

On the other hand, if σ_o is not connected to the boundary, there must be some spin- $\frac{1}{2}$ surrounding polygons enclosing the central site in addition to those from the boundary. Each of these polygons includes odd number of spin- $\frac{1}{2}$ states of $\alpha_1, \dots, \alpha_{N-1}$. The total contribution of each polygon, taking into account the weight from its orientation, is

$$e^\lambda e^{-(i\pi+2\lambda)/2} + e^{-\lambda} e^{(i\pi+2\lambda)/2} = 0 .$$

Thus $S(\alpha)$ counts the number of polygon configurations for which σ_o is connected to the boundary. We therefore have

$$\langle S(\alpha) \rangle = P = M . \quad (4.1.7)$$

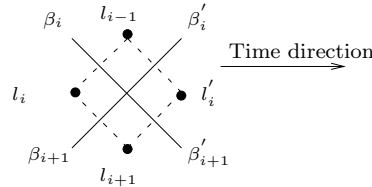
Having established the above equality we could investigate directly the spectrum of the relevant corner transfer matrix. There is however a faster way that uses already known results for solid on solid models.

4.2 The local height probability and spontaneous magnetization

The mapping between Γ_k vertex model and sos[22] is standard. Height variables l_i 's are assigned to faces separated by the arrow spins (see fig.(14)). The heights are given integer values consistent with

$$l_i - l_{i-1} = 2\beta_i \in \{k, k-2, \dots, -k\} \quad (4.2.1)$$

where l_i and l_{i-1} are heights of faces separated the spin arrow β_i . Each vertex is replaced by a square face with heights attached to the four corners and contributes to the partition function a weight $W(l_{i-1}, l_i, l_{i+1}, l'_i)$ which is set equal to the weight of the underlying vertex.



Figure(14) Vertex and sos correspondance

This sos model is a special case of the fused eight-vertex restricted solid on solid model(rsos)[23, 24]. The rsos model is integrable and is equivalent to the fusion of the eight-vertex model where heights can assume values from 1 to $L - 1$ besides the above constraint (4.2.1). In the limit[25]

$$\begin{aligned} L &\longrightarrow \infty \text{ and} \\ l_i &\longrightarrow \infty \text{ for all } i, \end{aligned} \quad (4.2.2)$$

such that relative heights of neighbouring faces remains unchanged, the sos model can be recovered from the rsos model. More precisely, the regime III of the rsos model corresponds to the $Q > 4$ range of the sos model in the above limit[26]. The Local height probability defined as[23]

$$P(a/b, c) = \frac{Z(a/b, c)}{\sum_{a=1}^{L-1} Z(a/b, c)} \quad (4.2.3)$$

has been computed exactly for the rsos model in the thermodynamics limit using the method of corner transfer matrix[24]. In this formula, $Z(a/b, c)$ denotes the rsos partition function with central height given by a , and b, c are heights of the faces at the boundary of the lattice that determine the state of the arrow spin on the perimeter (see fig.(13)). The lattice we considered has the b face separated from the a face (the central face) by even number of steps (see fig.(13)). In regime III, the rsos model has ground state configurations such that all faces separated by even steps assume the same value while all other faces assume another fixed value. The sos model has also the same ground state configurations since relative heights are not affected by the limit. A ground state is selected by fixing the heights b, c at the boundary.

Taking the above limit (4.2.2), the local height probability in the the thermodynamics limit has the expression

$$P(a/b, c) = \frac{x^{((b+c)/2-a)^2/2k} C_m^l}{\sum_{a=0}^{\infty} x^{((b+c)/2-a)^2/2k} C_m^l} \quad (4.2.4)$$

where

$$\begin{aligned} l &= (c - b + k)/2, \\ m &= (b + c)/2 - a + k/2 \text{ mod } 2k, \\ x &= e^{-2\lambda}, \end{aligned}$$

and $C_m^l(x)$ is the SU(2) level- k string function[27], which depends on λ and has the following properties

$$\begin{cases} C_m^l = 0 & \text{if } l \neq m \text{ mod } 2, \\ C_m^l = C_{m+2k}^l = C_{-m}^l, \\ C_m^l = C_{k-m}^{k-l} = C_{k+m}^{k-l}. \end{cases} \quad (4.2.5)$$

Notice that there is no dependence on the spectral parameter u , and C_m^l in the above formula is nonvanishing because a and b are on the same sublattice.

The spontaneous magnetization can now be computed by noting that the exponent in $S(\alpha)$ is

$$2(\alpha_1 + \dots + \alpha_{N-1}) = b - a$$

and making the substitution

$$S(\alpha) = e^{-(\lambda+i\pi/2)(b-a)}$$

which depends solely on the central height for given boundary condition. The expectation value therefore becomes

$$\langle S(\alpha) \rangle = \sum_{a=0}^{\infty} e^{-(\lambda+i\pi/2)(b-a)} P(a/b, c). \quad (4.2.6)$$

Replacing in the above formula m by $m + 2nk$ for

$$m = -k + 1, -k + 2, \dots, k$$

and

$$b - a = n \in \mathbf{Z},$$

the spontaneous magnetization becomes

$$M = \langle S(\alpha) \rangle = \frac{\sum_m \sum_n x^{2kn^2+2mn+m^2/2k+k/8-l/2} (-1)^{(m-l)/2+nk} C_m^l}{\sum_m \sum_n x^{2kn^2+(2m-k)n+(m-k/2)^2/2k} C_m^l}, \quad (4.2.7)$$

where

$$l = k, k - 1, \dots, 0$$

specifies the various boundary conditions. The formula can be expressed as finite sums of products of elliptic theta functions and string functions. Putting $k = 1$ into the above formula, we recover Baxter's[20] results for the spontaneous magnetization of the standard Potts model. For given k , we find $k + 1$ spontaneous magnetizations associated to the various boundary conditions of the vertex model. However, it is not difficult to show using (4.2.5) that whenever l is odd, $M = 0$. The latter condition is equivalent to

$$c - b = \begin{cases} k, k - 4, \dots, -k + 2 & \text{for odd } k, \\ k - 2, k - 6, \dots, -k + 2 & \text{for even } k, \end{cases} \quad (4.2.8)$$

Depending on the parity of k , there are thus $(k + 1)/2$ or $k/2$ vertex boundary conditions that actually give rise to vanishing magnetization. $M \neq 0$ for even l , ie.

$$l = \begin{cases} k - 1, k - 3, \dots, 0 & \text{for odd } k \\ k, k - 2, \dots, 0 & \text{for even } k \end{cases} \quad (4.2.9)$$

One then has

$$M = \frac{\sum_{m=-k+1}^k \theta_{\nu}(2mi\lambda, x^{2k}) x^{m^2/2k+k/8-l/2} (-1)^{(m-l)/2} C_m^l}{\sum_{m=-k+1}^k \theta_3((2m-k)i\lambda, x^{2k}) x^{(m-k/2)^2/2k} C_m^l} \quad (4.2.10)$$

with

$$\nu = \begin{cases} 4 & \text{for odd } k \\ 3 & \text{for even } k, \end{cases}$$

where the elliptic theta functions θ_ν are defined as

$$\begin{aligned}\theta_3(u, q) &= \sum_{n \in \mathbb{Z}} q^{n^2} e^{2niu} \\ \theta_4(u, q) &= \sum_{n \in \mathbb{Z}} (-1)^n q^{n^2} e^{2niu} .\end{aligned}$$

The above expressions are distinct for the various values of l . For example when $k = 2$, the results for $l = 0, 2$ have different behaviors in the large Q limit as shown below. With the help of the following approximation for the string functions[28]

$$C_{l+m}^l \stackrel{x \rightarrow 0}{\approx} \begin{cases} x^{-m^2/2k - ml/k} C_l^l (1 + O(x^2)) & m \leq 0 \\ x^{-m^2/2k - m(k-l)/k} C_l^l (1 + O(x^2)) & m > 0 \end{cases} \quad (4.2.11)$$

valid for $0 \leq l \leq k$, one finds that in the limit where Q approaches infinity, the spontaneous magnetizations for the various boundary conditions given by even l approach unity as follows

$$M \stackrel{\lambda \rightarrow \infty}{\approx} \begin{cases} 1 - 2x - x^2 + (x - x^2 + \delta_{k,1} x^2) \delta_{l,0} & \text{for odd } k , \\ 1 - 2x - x^2 + (x - x^2) \delta_{l,0} + x \delta_{l,k} & \text{for even } k . \end{cases} \quad (4.2.12)$$

Another limit to consider is $Q = 4^+$ or $\lambda = 0^+$ which divides the regions of first and second order transitions along the integrable line[29]. The expansion around $Q = 4$ can be obtained by employing the modular transformation formula of the string functions,

$$C_m^l(\tau) = \sqrt{\frac{\tau}{ik(k+2)}} \sum_{l'=0}^k \sum_{m'=-k+1}^k e^{i\pi m m' / k} \sin \left[\frac{\pi(l+1)(l'+1)}{k+2} \right] C_{m'}^{l'}(-1/\tau) \quad (4.2.13)$$

and that for the elliptic theta functions, which is standard. The parameter of the modular group in this case is $\tau = 2i\lambda/\pi$. Making the transformation and taking the limit leads to

$$M \stackrel{\lambda \rightarrow 0}{\approx} \begin{cases} \frac{e^{-(2k+1)\pi^2(Q-4)^{-1/2}/8(k+2)}}{2 \sin[\pi(l+1)/2(k+2)]} & \text{for odd } k \\ \frac{e^{-k\pi^2(Q-4)^{-1/2}/4(k+2)}}{\sin[\pi(l+1)/(k+2)]} & \text{for even } k . \end{cases} \quad (4.2.14)$$

Hence the magnetization vanishes with an essential singularity as $Q \rightarrow 4^+$. A numerical calculation of the spontaneous magnetization given in (4.2.10) shows that for given k and Q in the domain $[4, \infty]$, the spontaneous magnetizations are bounded from below and above by 0 and 1 as physically expected. Moreover they are ordered as follows

$$\begin{aligned} k \text{ odd} & \quad M_0 > M_{k-1} > M_2 > M_{k-3} > \cdots > M_{(k-1)/2} , \\ k \text{ even} & \quad M_k > M_0 > M_{k-2} > M_2 > \cdots > M_{k/2} . \end{aligned} \quad (4.2.15)$$

As in the construction of the models, we again observe a natural splitting between k odd and k even.

4.3 Conjectured phase diagram

We have computed spontaneous magnetizations in a rather formal fashion, and their meaning for $k > 1$ is not completely clear. The simplest possibility is to assume that, as in the $k = 1$ case, different vertex boundary conditions correspond indeed to different phases of the Γ_k Potts model. We shall then refer to the cases where $M = 0$ as disordered phases, although such phases may well have for instance antiferromagnetic order. Similarly ordered phase refers to $M \neq 0$. The order (4.2.15) suggests that such phases can be characterized by their degree of spin alignment.

We can then make some conjectures about the structure of the phase diagram of the family of Γ_k Potts model in the neighborhood of the JB integrable line (3.6.2) for $Q > 4$. We shall consider only the staggered Γ_k Potts model with lattice isotropy. This Potts model has k parameters f_i ; $i = 0, \dots, k-1$ which are introduced in the previous section. Recall that the JB integrable model is homogeneous and satisfies the condition (3.6.2), therefore the requirement of lattice isotropy fixes the spectral parameter u to be $\gamma/2$ and the JB integrable model corresponds to a point (denoted as P_{JB} in the sequel) in the k dimensional parameter space. We now wish to build, for fixed $Q > 4$, the phase diagram in the neighborhood of this integrable point, where the above calculation of spontaneous magnetization is performed. We expect that there are $k+1$ distinct phases, while k parameters are at our disposal. As for $k = 1$ we expect that these $k+1$ phases coexist only at P_{JB} . This implies that the phase diagram around P_{JB} has the topology of the dual of a k -simplex where each phase has a common boundary with any other phases. The boundaries that separate the phases can be deduced from the symmetry properties of the Potts model. The discussion again split into two cases; k odd and k even. For simplicity we just discuss two examples.

We start by the Γ_3 Potts model, which has two ordered and two disordered phases. The model has a duality transformation given by

$$f_0 \longleftrightarrow f_0^{-1}, \quad (4.3.1)$$

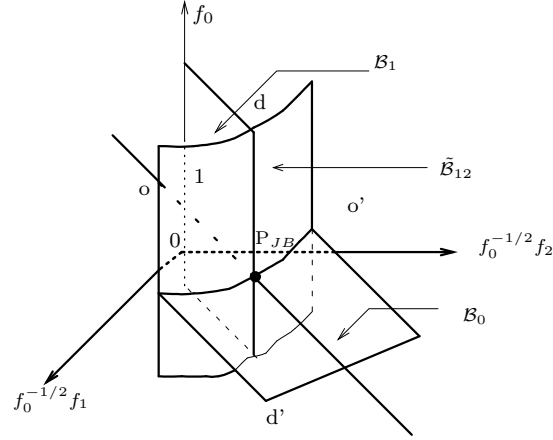
$$\text{and } f_0^{-1/2} f_1 \longleftrightarrow f_0^{-1/2} f_2. \quad (4.3.2)$$

We expect that duality still interchanges respectively ordered and disordered phases, and therefore that the boundaries of these four phases are invariant surfaces of the duality map. These surfaces have to be given by

$$\begin{aligned} \mathcal{B}_0 &: & f_0 - 1 &= 0, \\ \mathcal{B}_1 &: & f_1 - f_2 &= 0 \\ \text{and } \tilde{\mathcal{B}}_{12} &: & F(f_0^{-1/2} f_1, f_0^{-1/2} f_2) &= 0 \end{aligned} \quad (4.3.3)$$

where the unknown function F depends only on $f_0^{-1/2} f_1$ and $f_0^{-1/2} f_2$, and satisfies the following conditions

$$\begin{aligned} F(f_0^{-1/2} f_1, f_0^{-1/2} f_2) &= F(f_0^{-1/2} f_2, f_0^{-1/2} f_1), \\ \text{and } F(f_0^{-1/2} f_1, f_0^{-1/2} f_2) &= 0 \quad \text{at } P_{\text{JB}}. \end{aligned}$$



Figure(15) Phase diagram of the Γ_3 Potts model in the neighborhood of the JB integrable line point. The three surfaces $f_0 = 1$, $f_1 = f_2$ and $F = 0$ divide the four phases o, d, o', d' . The phase diagram has the topology that the four phases meet only at the integrable point P_{JB} .

Incorporating the fact that the phase diagram has the topology of the dual of a (degenerate) 3-simplex, we arrive at the phase diagram shown in fig.(15). The phases are grouped into two pairs (o, d) and (o', d') where $o(\prime)$ and $d(\prime)$ denote respectively the ordered and disordered phases that are exchanged under duality. Since spaces below and above \mathcal{B}_0 , and spaces on the left and right of \mathcal{B}_1 are interchanged by duality transformation, \mathcal{B}_0 and \mathcal{B}_1 are therefore the boundaries that separate o from d and o' from d' respectively. The boundary that divides these two pairs of phases is provided by the surface $\tilde{\mathcal{B}}_{12}$, which is symmetric in $f_0^{-1/2} f_1$ and $f_0^{-1/2} f_2$, and contains the integrable point P_{JB} .

Consider now the example of the Γ_2 Potts model. The parameters are f_0 and f_1 . Notice first that the model with face isotropy has only one parameter, f_1 , and thus cannot be expected to exhibit three phases in the neighborhood of the JB point. This means that face isotropy has to be spontaneously broken. There is no self duality, but simultaneous rotation of each of the fundamental blocks by 90° about its center interchanges ordered and disordered phases. Rotation of the fundamental blocks amounts to

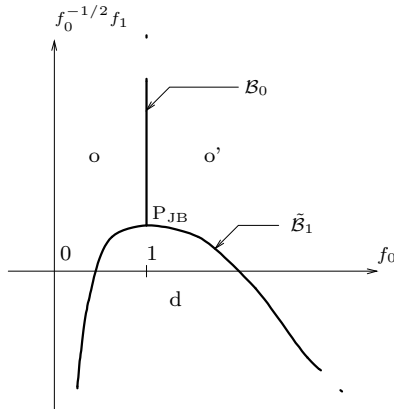
$$f_0 \longleftrightarrow f_0^{-1}.$$

There are two lines which are invariant under this transformation;

$$\begin{aligned} \mathcal{B}_0 &: f_0 - 1 = 0, \\ \tilde{\mathcal{B}}_1 &: G(f_0, f_1) = 0 \end{aligned} \tag{4.3.4}$$

where the function G satisfies

$$\begin{aligned} G(f_0, f_1) &= G(f_0^{-1}, f_1), \\ G(f_0, f_1) &= 0 \text{ at } P_{JB}, \\ \text{and } \left. \frac{\partial G}{\partial f_0} \right|_{P_{JB}} &= 0. \end{aligned}$$



Figure(16) Phase diagram the Γ_2 Potts model in the neighborhood of the JB integrable point. The three phases o, o', d are separated by \mathcal{B}_0 and $\tilde{\mathcal{B}}_1$, which are invariant curves under rotation of all the faces.

The typical phase diagram is shown in fig.(16).

Finally we want to remark that the above scenario relies upon the assumption that there is no other phase transition lines that bifurcate from the JB integrable line at some $Q \geq 4$. Recall that such phenomena occurs in the Ashkin-Teller model where the self dual line (where the underlying staggered vertex model becomes homogeneous) bifurcates into two phase transition lines.

5 The Γ_2 Model

While the models for $Q > 4$ are generally expected to be non critical, the phase diagrams for $Q < 4$ should exhibit several kinds of second order phase transitions. We shall here discuss in some details the case of Γ_2 . We restrict to the non staggered case (which would be the two lines $x^2 = 1$ in the Γ_1 case) and to the geometry of cylinder, ie. periodicity in time direction, with free boundary condition on the top and bottom rows. This ensures quantum group symmetry, which will turn out to be quite a useful ingredient. To start, we discuss the related one dimensional quantum spin chain.

5.1 The quantum spin chain

The hamiltonian can always be written as a general linear combination of the projectors as follows;

$$H = \sum_{i=1}^{2l-1} (\sin \omega - \cos \omega)(Q - 1)P_0(i, i + 1) - \cos \omega(Q - 2)P_1(i, i + 1) \quad (5.1.1)$$

where $P_j(i, i + 1)$'s are projectors that project onto the irreducible spin- j representation from the tensor product of the spin-1 states at sites i and $i + 1$, and the spin chain has free boundary conditions. We have chosen the coefficients of the projectors for later convenience. The parameter ω takes values in $[0, 2\pi]$ and q

is restricted to the case $|q| = 1$, we define as before $q = e^{i\gamma}$, $\gamma \in \mathbf{R}$ and introduce the parameter $\delta = \pi/\gamma$. Owing to the existence of the unitary transformation

$$UP_j(q)U^{-1} = P_j(-q^{-1}) \quad ; j = 0, 1, 2 \quad (5.1.2)$$

where

$$\begin{aligned} U = & \mathbf{1} + \frac{1}{2}S^z \otimes S^z - \frac{1}{2}S^{z^2} \otimes S^{z^2} - \frac{1}{4}S^{+2} \otimes S^{-2} - \frac{1}{4}S^{-2} \otimes S^{+2} \\ & + \beta S^+ S^z \otimes (1 - S^z)S^- + \beta^{-1}S^- S^z \otimes (S^z - 1)S^+ + \alpha S^+(1 + S^+) \otimes S^z S^- \\ & + \alpha^{-1}S^-(1 + S^z) \otimes S^z S^+ \quad ; \alpha, \beta \in \mathbf{C} \end{aligned}$$

and

$$S^+ = \begin{pmatrix} 0 & \sqrt{2} & 0 \\ 0 & 0 & \sqrt{2} \\ 0 & 0 & 0 \end{pmatrix}, \quad S^- = \begin{pmatrix} 0 & 0 & 0 \\ \sqrt{2} & 0 & 0 \\ 0 & \sqrt{2} & 0 \end{pmatrix}, \quad S^z = \begin{pmatrix} 1 & 0 & 0 \\ 0 & 0 & 0 \\ 0 & 0 & -1 \end{pmatrix}$$

are the usual $\mathfrak{su}(2)$ generators, it suffices to consider γ in the domain $[0, \pi/2]$. The hamiltonian is in general not hermitian with

$$H_i^\dagger(q) = H_i(q^{-1}), \quad (5.1.3)$$

however, through relabeling of the spin sites, $H_i(q^{-1})$ can be made equivalent to $H_i(q)$ and therefore the energy eigenvalues are real or occur in conjugate pairs. The hamiltonian can be written in terms of the more familiar $\mathfrak{su}(2)$ spin operators as,

$$\begin{aligned} H = & \sum_{i=1}^{2l-1} \{-2 \cos \omega \cos 2\gamma + \cos \omega - \sin \omega + \cos \omega \sigma_i + \sin \omega \sigma_i^2 + \sin^2 \gamma [(\sin \omega - \cos \omega)(\sigma_i^z - \sigma_i^{z^2}) \\ & - 2 \cos \omega (S_i^{z^2} + S_{i+1}^{z^2})] + \frac{i \sin 2\gamma}{2} (\sin \omega + \cos \omega) \sigma_i^z (S_i^z - S_{i+1}^z) + \frac{i \sin \gamma}{2} (\sin \omega + \cos \omega) \\ & [\sigma_i^\perp (S_i^z - S_{i+1}^z) + (S_i^z - S_{i+1}^z) \sigma_i^\perp] + (\sin \omega - \cos \omega) (\cos \gamma - 1) (\sigma_i^\perp \sigma_i^z + \sigma_i^z \sigma_i^\perp)\} \\ & + i \cos \omega \sin 2\gamma (S_1^z - S_{2l}^z) \end{aligned} \quad (5.1.4)$$

where

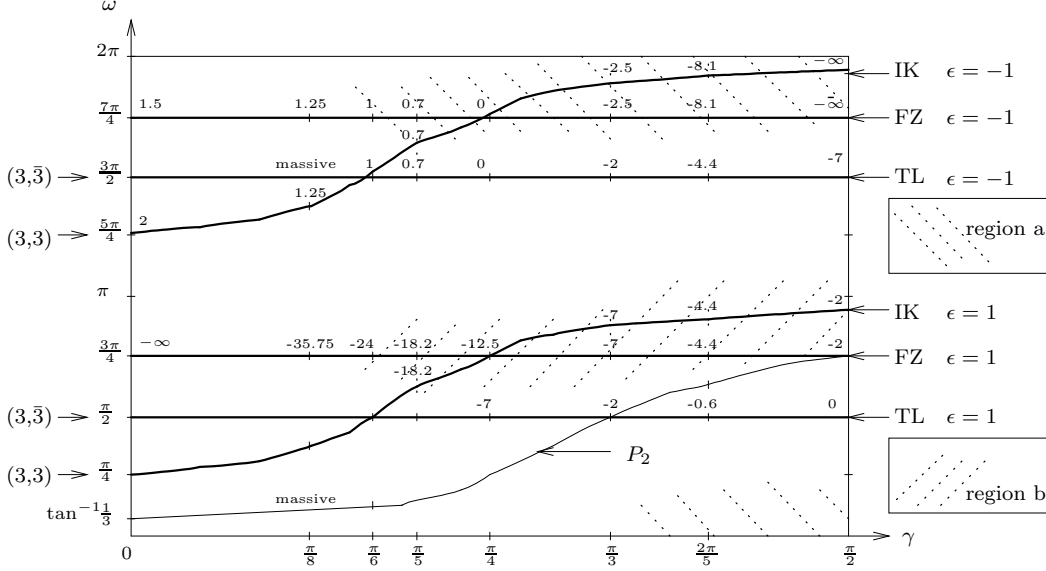
$$\begin{aligned} \sigma_i &= \vec{S}_i \cdot \vec{S}_{i+1} = \sigma_i^\perp + \sigma_i^z, \\ \sigma_i^z &= S_i^z S_{i+1}^z. \end{aligned}$$

Written in this manner, this hamiltonian can therefore be regarded as a special case of the spin-1 XXZ chain where the boundary terms ensure $U_q \mathfrak{su}(2)$ symmetry.

The hamiltonian reduces to that of the bilinear biquadratic spin chain with $\mathfrak{su}(2)$ symmetry at $\gamma = 0$ (or $q = 1$). It has the simple expression

$$H = \sum_{i=1}^{2l-1} [\cos \omega \sigma_i + \sin \omega \sigma_i^2]. \quad (5.1.5)$$

This model has a nontrivial phase diagram. We summarize in fig.(17) and below certain features of the phase diagram[30]:



Figure(17) Phase diagram of the Γ_2 spin chain. The various integrable lines have central charge given by

IK	$\epsilon = -1$	$c = \begin{cases} \frac{3}{2} - \frac{12}{\delta(\delta-2)} & ; \delta \in [2, 6) \\ 2 - \frac{6}{\delta} & ; \delta \in [6, \infty) \end{cases}$
FZ	$\epsilon = -1$	$c = \frac{3}{2} - \frac{12}{\delta(\delta-2)} ; \delta \in [2, \infty)$
TL	$\epsilon = -1$	$c = 1 - \frac{6}{\delta'(\delta'-1)} ; \delta \in [2, 6]$
		massive ; $\delta \in [6, \infty)$
IK	$\epsilon = 1$	$c = 1 - \frac{6(\delta-1)^2}{\delta} ; \delta \in [2, 6)$
FZ	$\epsilon = 1$	$c = 1 - \frac{6(\delta-1)^2}{\delta} ; \delta \in [2, \infty)$
TL	$\epsilon = 1$	$c = 1 - \frac{6}{\delta'(\delta'-1)} ; \delta \in [2, 4]$

where δ' is related to δ by $-2\epsilon \cos \frac{\pi}{\delta'} = 2 \cos \frac{2\pi}{\delta} + 1$. Some of these values are indicated in the figure.

The phase diagram is essentially divided into four regions $\omega \in (\frac{\pi}{2}, \frac{5\pi}{4}), (\frac{5\pi}{4}, \frac{3\pi}{2}), (\frac{3\pi}{2}, \frac{\pi}{4})$ and $(\frac{\pi}{4}, \frac{\pi}{2})$ depending on the ground state of the spin chain. For $\frac{\pi}{2} < \omega < \frac{5\pi}{4}$, the ground state is ferromagnetic. The model is integrable at $\omega = \frac{3\pi}{4}$ and has (formally) central charge $c = -\infty$. At the boundaries, $\omega = \frac{\pi}{2}$ and $\frac{5\pi}{4}$ the symmetry is augmented from $\mathfrak{su}(2)$ to $\mathfrak{su}(3)$. More specifically, at $\frac{\pi}{2}$, neighboring spins assume the representation $(\bar{3}, 3)$, the hamiltonian being proportional to $3P_0$ is related to the spin- $\frac{1}{2}$ Heisenberg antiferromagnetic spin chain via the Temperley Lieb algebra. At $\frac{5\pi}{4}$ neighboring spins belong to $(3, 3)$ representation, the spin chain is the permutation model studied by Sutherland *et al*[31] and is found to have central charge equal to 2. In the interval $\frac{5\pi}{4} < \omega < \frac{3\pi}{2}$, the spin chain is found using a semi classical approach to have vanishing magnetization but nonzero tensorial order parameter, the ground state therefore exhibits a "nematic order". At $\frac{3\pi}{2}$ the spin chain has hamiltonian $-P_0$ which differs from that at $\frac{\pi}{2}$ by a sign, it is again in the representation $(\bar{3}, 3)$. The ground state is found to have massive excitation. The interval $\frac{3\pi}{2} < \omega < \frac{\pi}{4}$, where we have identified the point $\omega = 0$ and 2π , has antiferromagnetic ground state and contains the Takhtajan-Babujian model[32] at $\omega = \frac{7\pi}{4}$, this point is solvable with $c = \frac{3}{2}$. In addition, the exact valence bond ground state[7] can be constructed at $\omega = \tan^{-1} \frac{1}{3}$, and the spin chain is shown to

have massive excitation. The vicinity of this point, which includes the Heisenberg antiferromagnetic model at $\omega = 0$, belongs to an antiferromagnetic fluid phase or disorder flat phase[33] where there is long range antiferromagnetic spin order and position disorder. For $\frac{\pi}{4} < \omega < \frac{\pi}{2}$, the ground state is dimerized, and at $\omega = \frac{\pi}{4}$, where phase transition occurs, the model is integrable and has $su(3)$ symmetry.

5.2 The Integrable Lines

The Γ_2 model has mainly been studied along the integrable lines (3.6.4),(3.6.9), (3.6.8), they are given, in terms of parameters of the spin chain, as

$$\begin{aligned} \text{(FZ)} \quad \tan \omega &= -1, \\ \text{(IK)} \quad \tan \omega &= \frac{1}{Q-3}, \\ \text{(TL)} \quad \cos \omega &= 0. \end{aligned}$$

The first two are related respectively to the $A_1^{(1)}$ and $A_2^{(2)}$ solutions to the Yang-Baxter equation[34], they have been studied first by Fateev-Zamolodchikov[35] and Izergin-Korepin[16]. The one labelled by TL has hamiltonian proportional to the spin-0 projector which is known to satisfy the Temperley-Lieb algebra[17]. We also want to point out that the FZ and TL lines are respectively the $k = 2$ element of the family of integrable models denoted as JB and TL in previous sections. Each of these equations gives rise to two lines in the $\omega - \gamma$ phase diagram where the hamiltonians differ by an overall sign. In the limit $\gamma = 0$, they reduce to the integrable points of the $su(2)$ invariant bilinear biquadratic spin chain. In this section, we shall examine the phase diagram beginning with these integrable lines, they will serve as benchmarks for the understanding of the critical properties of the general phase diagram. In fig.(17), we summarized the features of the phase diagram.

5.2.1 The TL case

It is governed by the hamiltonian

$$H = \epsilon \sum_{i=1}^{2l-1} (Q-1)P_0(i, i+1) \quad (5.2.1)$$

where

$$\epsilon = \begin{cases} 1 & \text{if } \omega = \pi/2, \\ -1 & \text{if } \omega = 3\pi/2. \end{cases}$$

The projectors $(Q-1)P_0$ satisfies the Temperley Lieb algebra (2.6) with

$$e_i = (Q-1)P_0$$

and

$$e_i^2 = (Q-1)e_i.$$

The corresponding vertex model has transfer matrix that satisfies the Yang-Baxter equation, the model is therefore integrable. In principle, energy eigenvalues and hence the critical properties can be deduced from

the Bethe anatz solution. However, we shall instead employ all that is known about the $U_q\text{su}(2)$ invariant spin- $\frac{1}{2}$ chain[6], which also has hamiltonian given by sum of Temperley Lieb generators, to understand this integrable case. Since the two hamiltonians are related to the same algebra, they share the same set of eigenvalues. On the other hand, as the representations are different, we do not expect the degeneracy to be identical. Also the same eigenvalue may appear in different spin sectors in the two models. To overcome these difficulties, we compare numerically their eigenvalues. It is worth pointing out that the hamiltonian has a hidden $U_q\text{sl}(3)$ symmetry[36] where neighboring spin sites are in the $(3, \bar{3})$ or $(\bar{3}, 3)$ representation of the quantum group, and P_0 can be regarded as the operator that projects the above representation onto the trivial representation.

The spin- $\frac{1}{2}$ $U_q\text{su}(2)$ invariant spin chain with free boundary condition has hamiltonian

$$H = - \sum_{i=1}^{2l-1} \sqrt{Q'} P_0(i, i+1) \quad (5.2.2)$$

it is the extreme anisotropic limit of the self dual six vertex model (2.16), and the projector $\sqrt{Q'} P_0$ satisfies the Temperley Lieb algebra with

$$e_i = \sqrt{Q'} P_0(i, i+1) .$$

The spin chain is critical for $\sqrt{Q'} \in [0, 2]$ (or $\delta' \in [2, \infty]$), and the central charge depends on δ' as[38]

$$c = 1 - \frac{6}{\delta'(\delta' - 1)} . \quad (5.2.3)$$

The ground state energy of spin- j sector ε_j^1 scales as[37]

$$\frac{l(\varepsilon_0^1 - \varepsilon_j^1)}{\xi\pi} \stackrel{l \rightarrow \infty}{\simeq} h_j \quad (5.2.4)$$

where

$$h_j = \frac{j[j(\delta' - 1) - 1]}{\delta'} \quad (5.2.5)$$

and the sound velocity

$$\xi = \frac{\delta'}{2} \sin \frac{\pi}{\delta'}$$

is obtained from the Bethe anatz solution[41]. For q a root of unity, the central charge belongs to the minimal series[39] with

$$c = 1 - \frac{6}{m(m+1)} \quad (5.2.6)$$

and $m = \delta' - 1$. The conformal weight is given by

$$h_{r,s} = \frac{[(m+1)r - ms]^2 - 1}{4m(m+1)} \quad (5.2.7)$$

and therefore

$$h_j = h_{1,1+2j} . \quad (5.2.8)$$

For $Q' > 4$, the spin chain is noncritical and has a massive excitation[1].

The spin- $\frac{1}{2}$ chain also has a ferromagnetic counter part[1], whose hamiltonian differs from (5.2.2) by an overall sign. The negated hamiltonian can in fact be obtained from (5.2.2) by rewriting the coefficient[6]

$$\sqrt{Q'} = -2 \cos(\pi(1 - \frac{1}{\delta'}))$$

and extending the domain of δ' to $[1,2]$ so that $(1 - \frac{1}{\delta'})^{-1} \in [2, \infty]$ or $-\sqrt{Q'} \in [0, 2]$. At $\sqrt{Q'} = 0$, it can be shown that the eigenvalues are symmetric about zero, the hamiltonian is therefore equivalent to its ferromagnetic counter part. We can therefore regard the ferromagnetic counter part as an extension of (5.2.2) where the domain of $\sqrt{Q'}$ is enlarged to include $[-2,0]$ or $\delta' \in [1, 2]$ as well. More importantly, it is found that for $\delta' \in [1, 2]$ the central charge and conformal weights are correctly given by (5.2.3) and (5.2.4), (5.2.5). In other words, the above results apply to the hamiltonian (5.2.2) with $\delta' \in [1, \infty]$.

At $\sqrt{Q'} = -2$, the spin chain is noncritical with $c = -\infty$, and for $\sqrt{Q'} \leq -2$, the ground state has massive excitation.

Comparing the hamiltonians (5.2.1) and (5.2.2), we see that the two spin chain have the same set of eigenvalues when

$$\sqrt{Q'} = \epsilon(1 - Q), \quad (5.2.9)$$

since the Temperley Lieb algebra realized by them have the same \sqrt{mQ} parameter. Numerical studies of the eigenvalues for the spin-1 chain of finite size ($2l < 10$) reveals that the spin-1 energy spectrum contains many crossing of eigenvalues due to the additional $U_{qsl}(3)$ symmetry. In particular we find,

$$\epsilon_{2j-1}^1 = \epsilon_{2j}^1 \quad \text{for } j \geq 1 \quad (5.2.10)$$

always hold. By comparing the ground state energies for various spin sectors of the spin- $\frac{1}{2}$ and spin-1 chain, we find, when Q' and Q are related by (5.2.9),

$$\begin{aligned} \epsilon = -1 & : \epsilon_{2j}^1 = \epsilon_j^{\prime 1} ; j \geq 0 \quad \text{for } Q \in [0, 4] \\ \epsilon = 1 & : \epsilon_{2j}^1 = \epsilon_j^{\prime 1} ; j \geq 0 \quad \text{for } Q \in [0, 2] \end{aligned} \quad (5.2.11)$$

where eigenvalues with prime belong to the spin- $\frac{1}{2}$ chain. For $\epsilon = -1$, this identification implies that the spin-1 chain is critical for $Q \in [0, 3]$, the central charge is given by (5.2.3) with δ' related to δ by (5.2.9) or

$$2 \cos \frac{\pi}{\delta'} = 2 \cos \frac{2\pi}{\delta} + 1,$$

and it increases from -7 to 1 as Q varies from 0 to 3. Moreover, the ground state of the spin- j sectors scales as

$$\frac{l(\epsilon_0^1 - \epsilon_{2j}^1)}{\xi\pi} \underset{N \rightarrow \infty}{\simeq} \frac{j[j(\delta' - 1) - 1]}{\delta'} \quad (5.2.12)$$

with the sound velocity given as before. Using (5.2.10), the scaling behavior of the odd spin sectors can also be deduced. Since $Q \in [3, 4]$ is mapped to the noncritical region $\sqrt{Q'} \in [2, 3]$ of the spin- $\frac{1}{2}$ chain, the spin-1 chain in this interval is therefore massive.

For $\epsilon = 1$, the identification is valid for $Q \in [0, 2]$ and the spin chain is critical with central charge given by (5.2.3) but in this case δ' and δ are related by

$$2 \cos \frac{\pi}{\delta'} = -1 - 2 \cos \frac{2\pi}{\delta} ,$$

hence the central charge varies from 0 to -7. For $Q \in [2, 4]$ the mapping (5.2.11) does not hold anymore, and it is not clear how to use the spin- $\frac{1}{2}$ chain to deduce the critical properties of the spin-1 model.

5.2.2 The FZ case

The FZ integrable spin chain has hamiltonian

$$H = \epsilon \sum_{i=1}^{2l-1} [2(Q-1)P_0(i, i+1) + (Q-2)P_1(i, i+1)] ; \quad \epsilon = \pm 1 , \quad (5.2.13)$$

it is the extreme anisotropic limit of the vertex model given in (3.6.2) for $k = 2$. For the $\epsilon = -1$ regime, the model is critical with central charge given by[42]

$$c = \frac{3}{2} - \frac{12}{\delta(\delta-2)} ; \quad \delta \in [2, \infty) , \quad (5.2.14)$$

while the lowest eigenvalue of each spin- j sector we found numerically to scale as

$$\frac{l(\epsilon_j^1 - \epsilon_0^1)}{\xi\pi} = \frac{j((\delta-2)j-2)}{2\delta} + \frac{1}{2}\delta_{j,\text{odd}} \quad (5.2.15)$$

where

$$\xi = \frac{\pi \sin 2\delta}{2\delta}$$

denotes the sound velocity. For q a root of unity, δ becomes rational, the central charge belongs to the superconformal series[40] where the conformal weight reads

$$h_{p,q} = \frac{(p\delta - q(\delta-2))^2 - 4}{8\delta(\delta-2)} + \frac{1}{32}[1 - (-1)^{p-q}] . \quad (5.2.16)$$

Substituting $p = 1$ and $q = 2j + 1$ into the above,

$$h_{1,2j+1} = \frac{j((\delta-2)j-2)}{2\delta} , \quad (5.2.17)$$

we recover (5.2.15) except for the additional term $\frac{1}{2}\delta_{j,\text{odd}}$. The spin chain is therefore related to the Neveu-Schwarz sector of the minimal superconformal series for q a root of unity. Furthermore, only the lowest eigenvalues of the even spin sectors are related simply to the primary states $|h_{1,i+2j} \rangle$, while for the odd spin sectors they are related to $G_{-\frac{1}{2}}|h_{1,i+2j} \rangle$ where $G_{-\frac{1}{2}}$ is the fermionic raising generator of the global superconformal group $\text{OSP}(2|1)$. This extra factor accounts for the term $\frac{1}{2}\delta_{j,\text{odd}}$ in (5.2.15). Another interesting phenomena occurs at the point $\gamma = \frac{\pi}{4}$. It has been noted that the numerical estimate of the

central charge is exactly zero and does not suffer from finite size correction. This point is related in fact to the $N = 2$ supersymmetric series[15].

The $\epsilon = 1$ regime of the FZ line has drastically different behavior from its $\epsilon = -1$ counterpart[43]. It has been studied for toroidal boundary conditions where

$$S_{2l+1}^{\pm} = e^{\pm i\phi} S_1^{\pm}, \quad S_{2l+1}^z = S_1^z.$$

The "effective" central charge depends also on ϕ as

$$c = 1 - \frac{3\phi^2}{2\pi\gamma}; \quad \gamma \in [0, \frac{\pi}{2}]. \quad (5.2.18)$$

It is however well known that with appropriate value for ϕ , this formula gives the central charge for the free boundary spin chain[11, 44]. Indeed, putting $\phi = 2\pi - 2\gamma$, we get

$$c = 1 - \frac{6(\delta - 1)^2}{\delta}; \quad \delta \in [2, \infty]. \quad (5.2.19)$$

This expression is the same as that for the spin- $\frac{1}{2}$ $U_{qsu}(2)$ invariant spin chain in the domain $\delta' \in [1, 2]$ as can be seen by replacing δ' by $\frac{\delta'}{\delta'-1}$ in (5.2.3). We have also verified numerically for the $\epsilon = 1$ FZ line that the ground state energy scales according to

$$\frac{l(\varepsilon_j^1 - \varepsilon_0^1)}{\xi\pi} = \frac{j(j - \delta + 1)}{\delta} \quad (5.2.20)$$

where

$$\xi = \frac{\pi \sin 2\delta}{2\pi - 2\delta}.$$

The above formula is in fact equal to (5.2.5) after the replacement

$$\delta' \longrightarrow \frac{\delta'}{\delta' - 1}.$$

This regime is therefore in the same universality class as the spin- $\frac{1}{2}$ chain (5.2.2) in the interval $\delta' \in [1, 2]$.

5.2.3 The IK case

The IK integrable spin chain has hamiltonian given by

$$H = \frac{\epsilon}{\sqrt{1 + (Q - 3)^2}} \sum_{i=1}^{2l-1} [(4 - Q)(Q - 1)P_0(i, i + 1) + (3 - Q)(Q - 2)P_1] \quad (5.2.21)$$

where $\epsilon = 1$ corresponds to

$$\omega = \tan^{-1}\left(\frac{1}{Q - 3}\right) \in [0, \pi]$$

and $\epsilon = -1$ to

$$\omega = \tan^{-1}\left(\frac{1}{Q-3}\right) + \pi.$$

The model coincides with the FZ chain at $\gamma = \frac{\pi}{4}$ and the TL chain at $\gamma = \frac{\pi}{6}$. Exact Bethe ansatz solution has been worked out for the model with toroidal boundary condition[45]. It was found that the critical behaviors are classified according to the following regimes;

$$\begin{aligned} \text{regime I} \quad \epsilon &= 1 & c &= 1 - \frac{3\phi^2}{2\pi\gamma} & ; \gamma &\in (0, \frac{\pi}{2}) \\ \text{regime II} \quad \epsilon &= -1 & c &= \frac{3}{2} - \frac{3\phi^2}{\pi(\pi-2\gamma)} & ; \gamma &\in (\frac{\pi}{6}, \frac{\pi}{2}) \\ \text{regime III} \quad \epsilon &= -1 & c &= \begin{cases} 2 - \frac{3\phi^2}{2\pi\gamma} & \phi \leq 2\gamma \\ -1 + \frac{3(\phi-\pi)^2}{\pi(\pi-2\gamma)} & \phi \geq 2\gamma \end{cases} & ; \gamma &\in (0, \frac{\pi}{6}); \end{aligned} \quad (5.2.22)$$

As in the previous case, these results can be used to obtain the central charge for the free boundary spin chain. We verify numerically that in regime II the central charge is given by $\phi = 2\gamma$ where the above formula becomes

$$c = \frac{3}{2} - \frac{12}{\delta(\delta-2)} \quad ; \delta \in (2, 6). \quad (5.2.23)$$

This expression is identical to (5.2.14) of the $\epsilon = 1$ FZ line. Moreover, numerical check of the energy eigenvalues shows that the ground state of each spin- j sector scales as (5.2.15) but with the sound velocity given in this case, following [45] by

$$\xi = \frac{2\pi \sin 2\gamma \cos 3\gamma}{(\pi - 6\gamma)\sqrt{Q + Q(Q-3)^2}}.$$

We therefore conclude that regime II is in the same universality class as the $\epsilon = -1$ FZ line for $\gamma \in (\frac{\pi}{6}, \frac{\pi}{2})$. However beyond $\gamma = \frac{\pi}{6}$ ie. regime III, the IK model has different critical behavior. Our numerical checks of the conformal weight proved inconclusive due to poor finite size convergence. On the other hand, it is known that the spin chain at $\gamma = 0$ is related to the permutation model studied by Sutherland *et al* where $c = 2$ and to TL model at $\gamma = \frac{\pi}{6}$ where $c = 1$. It is therefore likely that regime III has

$$c = 2 - \frac{6}{\delta} \quad (5.2.24)$$

which is obtained from above with the substitution $\phi = 2\gamma$. As for regime I, numerical check suggests again that the critical properties are again different in the two regimes

$$\begin{aligned} \text{regime I}' \quad \epsilon &= 1 & \gamma &\in (0, \frac{\pi}{6}) \\ \text{regime I}'' \quad \epsilon &= 1 & \gamma &\in (\frac{\pi}{6}, \frac{\pi}{2}). \end{aligned}$$

In regime I'', the model is found to be in the same universality class as the $\epsilon = -1$ FZ line where the central charge has expression (5.2.19) which is obtained from the above by taking $\phi = 2\pi - 2\gamma$, and the scaling behavior of the energy eigenvalues is given as in (5.2.20) with sound velocity

$$\xi = -\frac{2\pi \sin 2\gamma \cos 3\gamma}{3(\pi - 2\gamma)\sqrt{Q + Q(Q-3)^2}}.$$

for regime I', finite size convergence is poor and classification of the regime is uncertain.

It is intriguing to find that the IK and FZ line in both $\epsilon = \pm 1$ have the same critical properties for $\gamma \in (\frac{\pi}{6}, \frac{\pi}{2})$. To elucidate this we performed further numerical study for models "in between". The sound velocities are not known then, and the difference of ground state energies $\varepsilon_j^1 - \varepsilon_0^1$ is more difficult to use to deduce the critical behavior (such as (5.2.15)) of the model. One can still study quantities that do not depend on the sound velocity and compare them with the FZ and IK integrable cases. For given γ in the shaded regions a and b in fig.(17), we found that such scaled quantities approach those common to the two integrable lines as l increases. Further, the ordering of levels with respect to j is the same as that of the integrable lines. This behavior suggests that the shaded regions are massless phases, with the same universality class as the integrable lines. Other indications come from the fact that on the integrable lines, the ground state energies of certain spin sectors coincide at special values of γ such as

$$\begin{aligned} \epsilon = -1 \quad \delta\varepsilon_1^1(\frac{2\pi}{5}) &= \delta\varepsilon_3^1(\frac{2\pi}{5}), \\ \delta\varepsilon_1^1(\frac{\pi}{4}) &= \delta\varepsilon_2^1(\frac{\pi}{4}), \end{aligned} \quad (5.2.25)$$

and

$$\begin{aligned} \epsilon = 1 \quad \delta\varepsilon_1^1(\frac{\pi}{5}) &= \delta\varepsilon_3^1(\frac{\pi}{5}), \\ \delta\varepsilon_1^1(\frac{\pi}{4}) &= \delta\varepsilon_2^1(\frac{\pi}{4}), \\ \delta\varepsilon_0^1(\frac{\pi}{4}) &= \delta\varepsilon_3^1(\frac{\pi}{4}), \end{aligned} \quad (5.2.26)$$

which can be seen from (5.2.15) and (5.2.5) respectively. Numerical study shows that such crossings still hold in the shaded regions. Finally at $\gamma = \frac{\pi}{4}$ in region a, moving away from the integrable lines along the ω direction, the central charge is found to be exactly zero without finite size correction as in the integrable cases. A study of the operator contents of the continuum theories on the FZ line suggests that the operator of the $N = 1$ supersymmetric series that correspond to perturbing spin chain from the FZ line in the ω direction and which respect the quantum group symmetry of the spin chain has conformal weight $h_{3,1} = (\delta+2)/(2\delta-4)$ ie is irrelevant for $\gamma > \pi/6$ (region a). As for region b, it is likely that the operator of the minimal series that drives the perturbation from the integrable line as again weight $h_{3,1} = 2\delta - 1$, ie is irrelevant for $\gamma \in [0, \pi/2]$.

5.3 P_2 projector and the q -deformed valence bond states

Besides the integrable lines, the hamiltonian obtained by summing projectors $P_2(i, i+1)$ deserves further examination. Recall that for $q = 1$, the ground state of vanishing energy could be exactly constructed using Valence Bond States [7]. It turns out that the construction generalizes to arbitrary q . We shall again refer to the corresponding state as VBS. Notice that for $q = e^{i\gamma}$, such a state needs not always be the ground state. We shall in fact observe other eigenenergies crossing 0 as γ deviates from zero.

The hamiltonian considered lies along the line

$$\tan \omega = \frac{1}{Q-1} \quad ; \quad \omega \in [0, \pi] \quad (5.3.1)$$

with

$$H = \sum_{i=1}^{N-1} (Q-1)(Q-2)P_2(i, i+1), \quad (5.3.2)$$

where we have dropped an overall positive coefficient and a constant term. This restricts to the ($q = 1$) su(2) invariant model as a special case. Let us now extend the valence bond state method, used so far for the su(2) model, to the above hamiltonian. As a first step, we regard the spin-1 state $\psi_{\alpha\beta}$ as being formed by the q - symmetric product of two spin- $\frac{1}{2}$ states defined as

$$\psi_{\alpha\beta} = g_{\alpha\beta}\phi_\alpha \otimes \phi_\beta + g_{\beta\alpha}\phi_\beta \otimes \phi_\alpha \quad ; \quad \alpha, \beta = 1, 2 \quad (5.3.3)$$

where $g_{\alpha\beta}$ is the matrix element of

$$g = \begin{pmatrix} \frac{1}{\sqrt{2}} & \frac{\sqrt{2}q^{\frac{1}{2}}}{q+q^{-1}} \\ \frac{\sqrt{2}q^{-\frac{1}{2}}}{q+q^{-1}} & \frac{1}{\sqrt{2}} \end{pmatrix},$$

and ϕ_α denotes the orthonormal basis of the spin- $\frac{1}{2}$ states. The spin-1 state $\psi_{\alpha\beta}$ is by construction symmetric in the two indices α, β and is related to the orthonormal basis $|\pm\rangle, |0\rangle$ as

$$\psi_{11} = \sqrt{2}|+\rangle, \psi_{22} = \sqrt{2}|-\rangle, \psi_{12} = \psi_{21} = \sqrt{\frac{2}{q+q^{-1}}}|0\rangle.$$

Note that in our notation, the two spin- $\frac{1}{2}$ states are labelled by 1,2, and the three spin-1 states are labelled by $\pm, 0$. Consider two neighboring spin-1 states $\psi_{\alpha\alpha_1}$ and $\psi_{\beta_1\beta}$, we construct a tensor product using two of the spin- $\frac{1}{2}$ states (one from each spin-1 state) such that the total spin can only be 0 or 1, this is achieved with the help of the tensor

$$\epsilon = \begin{pmatrix} 0 & q^{-1} \\ -q & 0 \end{pmatrix} \quad (5.3.4)$$

and the tensor product is defined as

$$\Omega_{\alpha\beta} = \sum_{\alpha_1, \beta_1} \psi_{\alpha\alpha_1} \epsilon_{\alpha_1\beta_1} \psi_{\beta_1\beta}. \quad (5.3.5)$$

In the $q = 1$ case, ϵ reduces to the usual antisymmetric tensor with $\epsilon_{12} = 1$. One can check that the resulting element indeed belongs to the $U_q\text{su}(2)$ spin 1 representation by expressing the above as

$$\begin{aligned} \Omega_{11} &= \frac{-2}{\sqrt{q+q^{-1}}}(q^2+q^{-2})^{\frac{1}{2}}|1, 1\rangle, \\ \Omega_{22} &= \frac{-2}{\sqrt{q+q^{-1}}}(q^2+q^{-2})^{\frac{1}{2}}|1, -1\rangle, \\ q\Omega_{12} + q^{-1}\Omega_{21} &= -2(q^2+q^{-2})^{\frac{1}{2}}|1, 0\rangle \\ \text{and} \quad \Omega_{12} - \Omega_{21} &= 2(q^2+1+q^{-2})^{\frac{1}{2}}|0, 0\rangle \end{aligned} \quad (5.3.6)$$

where $\{|1, \pm\rangle, |1, 0\rangle\}$ and $\{|0, 0\rangle\}$ are respectively the orthonormal basis of the irreducible spin-1 and spin-0 representations, which are constructed out of two copies of spin-1 (four copies of spin 1/2) orthonormal bases from sites i and $i+1$ as follows

$$\begin{aligned} \text{spin-0 :} \quad |0, 0\rangle &= (q^2+1+q^{-2})^{-\frac{1}{2}}(q^{-1}|+-\rangle - |00\rangle + q| - + \rangle) \\ \text{spin-1 :} \quad |1, 1\rangle &= (q^2+q^{-2})^{-\frac{1}{2}}(q|0+\rangle - q^{-1}|+0\rangle) \\ |1, 0\rangle &= (q^2+q^{-2})^{-\frac{1}{2}}(|-+\rangle + (q-q^{-1})|00\rangle) - |+-\rangle \\ |1, -1\rangle &= (q^2+q^{-2})^{-\frac{1}{2}}(q|-0\rangle - q^{-1}|0-\rangle). \end{aligned} \quad (5.3.7)$$

These formulae show the important fact that the tensor product (5.3.5) satisfies

$$P_2(i, i+1)\Omega_{\alpha\beta} = 0. \quad (5.3.8)$$

Such a construction can be extended to the whole spin chain by tensoring neighboring spin-1 states with ϵ giving

$$\Omega_{\alpha\beta}^{(N)} = \sum_{\substack{\alpha_i \\ i \in [2, N]}} \sum_{\substack{\beta_j \\ j \in [1, N-1]}} \psi_{\alpha\beta_1} \epsilon_{\beta_1\alpha_2} \psi_{\alpha_2\beta_2} \cdots \epsilon_{\beta_{N-1}\alpha_N} \psi_{\alpha_N\beta} \quad (5.3.9)$$

the VBS state. It satisfies

$$H\Omega_{\alpha\beta}^{(N)} = 0 \quad (5.3.10)$$

which can be checked by considering the action of individual $P_2(i, i+1)$.

For the chain with free boundary conditions, the indices α, β give rise to four states which, when expressed as linear combination of strings of $|\pm\rangle, |0\rangle$, have the characteristic that a nonzero state $|+\rangle$ ($|-\rangle$) must be followed by a $|0\rangle$ or $|-\rangle$ ($|+\rangle$). Thus $|+\rangle$ and $|-\rangle$ appear alternately in the VBS and there can be any number of $|0\rangle$ between the $|+\rangle$ and $|-\rangle$. The four states are distinguished by the following

Ω_{11}^N The first nonzero states is $|+\rangle$ and the number of $|+\rangle$ states exceeds that of the $|-\rangle$ states by 1.

Ω_{12}^N The string has equal number of $|+\rangle$ and $|-\rangle$ states or all $|0\rangle$ states.

Ω_{21}^N Same as in the Ω_{12} case.

Ω_{22}^N Same as in the Ω_{11} case with $|+\rangle$ replaced by $|-\rangle$.

From the lattice gas point of view (where $|0\rangle$ is regarded as a vacancy), the VBS exhibits a perfect antiferromagnetic order and positional disorder.

Since Ω_{11}^N (Ω_{22}^N) contains an extra $|+\rangle$ ($|-\rangle$), we have,

$$\begin{aligned} S^z \Omega_{11}^N &= \Omega_{11}^N, \\ S^z \Omega_{22}^N &= -\Omega_{22}^N, \\ \text{and } S^z \Omega_{12(21)}^N &= 0. \end{aligned} \quad (5.3.11)$$

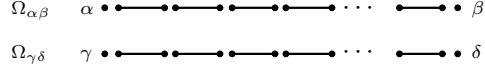
As in the $q = 1$ case, it can be proved that the four states belongs to the spin-0 and spin-1 irreducible representations, namely,

$$\begin{aligned} \Omega_{11}^N &\propto |1, 1\rangle, \\ \Omega_{22}^N &\propto |1, -1\rangle, \\ q\Omega_{12}^N + q^{-1}\Omega_{21}^N &\propto |1, 0\rangle \\ \text{and } \Omega_{12}^N - \Omega_{21}^N &\propto |0, 0\rangle. \end{aligned}$$

The norm can also be computed. We define scalar products by treating q formally as a real parameter so that the conjugate of the raising operator is the lowering operator, and vice versa. As an example the state

$$q|+\rangle + q^{-1}|-\rangle$$

has norm $q^2 + q^{-2}$ instead of 2. With this convention, eigenstates with different eigenvalues continue to be orthogonal for complex q . But we lose positivity and definiteness in general. The computation is now done using graphical means which generalize the method of [7]. The contraction $(\Omega_{\gamma\delta}^{(N)}, \Omega_{\alpha\beta}^{(N)})$ is represented graphically as two parallel series of horizontal links and dots (see fig.(18))



Figure(18) Graphical representation of the valence bond states

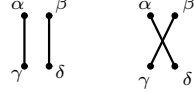
where each pair of closely spaced dots represents the two spin- $\frac{1}{2}$ states at each spin-1 site and the horizontal links represent the presence of the valence bond, ie. the ϵ tensor. Each pair of dots has contraction only with that directly below (or above) it, which gives the contraction of the spin-1 states from $\Omega_{\alpha\beta}^{(N)}$ and $\Omega_{\gamma\delta}^{(N)}$ at the same sites. We first examine the one particle norm

$$(\psi_{\gamma\delta}, \psi_{\alpha\beta}) = K_{\alpha\beta}(\delta_{\alpha\gamma}\delta_{\beta\delta} + \delta_{\alpha\delta}\delta_{\beta\gamma}) \quad (5.3.12)$$

where

$$K_{\alpha\beta} = g_{\alpha\beta}^2 + g_{\beta\alpha}^2.$$

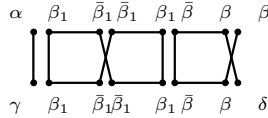
The rhs of (5.3.12) can be represented graphically as (figs.(19a)(19b))



Figure(19a) **Figure(19b)**

Contraction of two spin-1 states

and we shall refer to these two geometrical objects as the **parallel** and **crossed** vertical links respectively. It is now clear that $(\Omega_{\gamma\delta}^{(N)}, \Omega_{\alpha\beta}^{(N)})$ gives 2^N possible graphs which are obtained by replacing each of the one particle contraction by fig.(19a) or fig.(19b). A typical graph for $N = 4$ looks like



Figure(20) Typical graph for $N=4$

which carries a weight

$$\sum_{\beta_1} \delta_{\alpha\beta} K_{\alpha\beta_1} (\epsilon_{\beta_1\bar{\beta}_1}^2 \epsilon_{\bar{\beta}_1\beta_1}^2) K_{\bar{\beta}_1\beta_1} (\epsilon_{\bar{\beta}\beta}^2 \delta_{\beta\delta})$$

and we have introduced the notation

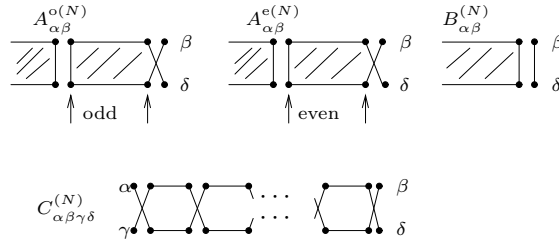
$$\bar{\beta} = \begin{cases} 1 & \text{if } \beta = 2, \\ 2 & \text{if } \beta = 1. \end{cases}$$

Our task now is to sum up the weights of the 2^N graphs. Unlike the $q = 1$ model where the sum can be performed using combinatoric arguments only, the q dependence of $K_{\alpha\beta}$ and ϵ complicates this approach and the sum has to be done with the help of recursion relations.

We shall define the collection of horizontal or vertical links which are connected together as a **circuit**, thus each graph is made up of disconnected circuits. Notice that the circuits come in two different forms, which are distinguished by the type of vertical links at the right and left most ends. In the above example, there are three disconnected circuits; The one in the middle has its rightmost vertical link formed by one of the parallel vertical links fig.(19a), while the circuit on the right has its rightmost vertical link given by fig.(19b) and left most link given by fig.(19a). We shall refer to them as circuits of type A and B respectively, note that in our definition, circuit of type B is characterized by the vertical links at its two ends, while circuit of type A by its rightmost end only. We also introduce the notion of length for these circuits, namely the length of a circuit is equal to half of the number of valence bond it covers. Therefore the B and A circuits in the example have length 2 and 1 respectively. Having established the notations, we are in a position to characterize the graphs. Any graph belong to one of the following types:

$$\begin{aligned}
\delta_{\alpha\gamma}\delta_{\beta\delta}A_{\alpha\beta}^{o(N)} & : \text{ graphs whose rightmost circuit is an odd length type A circuit,} \\
\delta_{\alpha\gamma}\delta_{\beta\delta}A_{\alpha\beta}^{e(N)} & : \text{ graphs whose rightmost circuit is an even length type A circuit,} \\
\delta_{\alpha\gamma}\delta_{\beta\delta}B_{\alpha\beta}^{(N)} & : \text{ graphs whose rightmost circuit is type B,} \\
C_{\alpha\beta\gamma\delta}^{(N)} & : \text{ graph which does not contain any parallel vertical link given in fig.(21).}
\end{aligned}$$

In the above definitions, N denotes the size of the spin chain, e and o denote the parity of the rightmost circuit. It is not difficult to see that the above four cases exhaust all the possible types of graph and are mutually exclusive. Among the 2^N graphs, only one of them is of type $C_{\alpha\beta\gamma\delta}^{(N)}$, it is made up two disconnected circuits running from one end of the graph to the other as given by the last figure in fig.(21). Since the first three types of graphs always come with the factor $\delta_{\alpha\gamma}\delta_{\beta\delta}$, we explicitly separate the factor from the rest of the contribution. Graphically these four types of graphs have the following features (fig.(21))

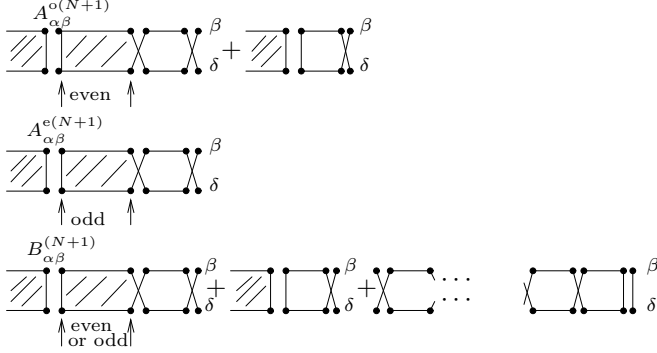


Figure(21) The four types of graphs

The weight $A^{(N)}$, $B^{(N)}$, $C^{(N)}$ of N sites can be related to that of $N + 1$ sites as

$$\begin{aligned}
A_{\alpha\beta}^{o(N+1)} & = A_{\alpha\bar{\beta}}^{e(N)} \epsilon_{\bar{\beta}\beta}^2 + B_{\alpha\bar{\beta}}^{(N)} \epsilon_{\bar{\beta}\beta}^2, \\
A_{\alpha\beta}^{e(N+1)} & = A_{\alpha\bar{\beta}}^{o(N)} \epsilon_{\bar{\beta}\beta}^2, \\
B_{\alpha\bar{\beta}}^{(N+1)} & = \sum_{\beta_1} (A_{\alpha\beta_1}^{e(N)} \epsilon_{\beta_1\bar{\beta}_1}^2 K_{\bar{\beta}_1\beta} + A_{\alpha\beta_1}^{o(N)} \epsilon_{\beta_1\bar{\beta}_1}^2 K_{\bar{\beta}_1\beta} + B_{\alpha\beta_1}^{(N)} \epsilon_{\beta_1\bar{\beta}_1}^2 K_{\bar{\beta}_1\beta}) \\
& \quad + \epsilon_{\alpha\bar{\alpha}}^2 K_{\bar{\alpha}\beta} \delta_{N,\text{odd}} + K_{\alpha\beta} \delta_{N,\text{even}},
\end{aligned} \tag{5.3.13}$$

which correspond to the various ways of appending an additional site to the N -site graphs (see fig.(22))



Figure(22) Graphical representation of the recursion relations (5.3.13).

The weight of $C_{\alpha\beta\gamma\delta}^{(N)}$ can be calculated directly as

$$C_{\alpha\beta\gamma\delta}^{(N)} = \begin{cases} (K_{\alpha\gamma})^{N-1} K_{\beta\delta} \epsilon_{\alpha\beta} \epsilon_{\gamma\delta} & ; N \in \text{even} , \\ (K_{\alpha\gamma})^N \delta_{\alpha\delta} \delta_{\gamma\beta} & ; N \in \text{odd} . \end{cases} \quad (5.3.14)$$

The set of recursion relations (5.3.13) can be solved easily when they are iterated once to relate graphs whose length are of the same parity. This gives, for N odd,

$$\begin{aligned} A_{\alpha\beta}^{o(N+2)} &= A_{\alpha\beta}^{o(N)} + \sum_{\beta_1} (A_{\alpha\beta_1}^{o(N)} \tilde{K}_{\beta_1\beta} + A_{\alpha\beta_1}^{e(N)} \tilde{K}_{\beta_1\beta} + B_{\alpha\beta_1}^{(N)} \tilde{K}_{\beta_1\beta}) + \tilde{K}_{\alpha\beta} , \\ A_{\alpha\beta}^{e(N+2)} &= A_{\alpha\beta}^{e(N)} + B_{\alpha\beta}^{(N)} , \\ B_{\alpha\beta}^{(N+2)} &= \sum_{\beta_1} (A_{\alpha\beta_1}^{o(N)} K_{\beta_1\beta} + A_{\alpha\beta_1}^{e(N)} K_{\beta_1\beta} + B_{\alpha\beta_1}^{(N)} \tilde{K}_{\beta_1\beta} + \sum_{\alpha_1} (A_{\alpha\alpha_1}^{o(N)} \tilde{K}_{\alpha_1\beta_1} K_{\beta_1\beta} \\ &\quad + A_{\alpha\alpha_1}^{e(N)} \tilde{K}_{\alpha_1\beta_1} K_{\beta_1\beta} + B_{\alpha\alpha_1}^{(N)} \tilde{K}_{\alpha_1\beta_1} K_{\beta_1\beta}) + \tilde{K}_{\alpha\beta_1} K_{\beta_1\beta}) + K_{\alpha\beta} . \end{aligned} \quad (5.3.15)$$

where

$$\tilde{K}_{\alpha\beta} = \epsilon_{\alpha\bar{\alpha}}^2 K_{\alpha\beta} \epsilon_{\bar{\beta}\beta}^2 .$$

The above may be written more compactly as the matrix equation

$$\mathbf{G}^{(N+2)} + \mathbf{1} = (\mathbf{G}^{(N)} + \mathbf{1})(\mathbf{1} + \tilde{\mathbf{K}})(\mathbf{1} + \mathbf{K}) \quad (5.3.16)$$

where

$$\mathbf{G}^{(N)} = \mathbf{A}^{o(N)} + \mathbf{A}^{e(N)} + \mathbf{B}^{(N)}$$

is a 2×2 matrix whose indices are labelled by α and β , and from the definition, it includes $2^N - 1$ graphs, the missing one being $C_{\alpha\beta\gamma\delta}^{(N)}$.

For N even, similar calculation gives

$$\tilde{\mathbf{G}}^{(N+2)} + \mathbf{1} = (\tilde{\mathbf{G}}^{(N)} + \mathbf{1})(\mathbf{1} + \mathbf{K})(\mathbf{1} + \tilde{\mathbf{K}}) \quad (5.3.17)$$

where

$$\tilde{G}_{\alpha\beta}^{(N)} = G_{\alpha\bar{\beta}}^{(N)} \epsilon_{\bar{\beta}\beta}^2 .$$

Equations (5.3.16), (5.3.17) lead to the results

$$\begin{aligned}\mathbf{G}^{(N)} &= (\mathbf{1} + \mathbf{K})[(\mathbf{1} + \tilde{\mathbf{K}})(\mathbf{1} + \mathbf{K})]^{\frac{N-1}{2}} - \mathbf{1} & N \in \text{odd} , \\ \tilde{\mathbf{G}}^{(N)} &= [(\mathbf{1} + \mathbf{K})(\mathbf{1} + \tilde{\mathbf{K}})]^{\frac{N}{2}} - \mathbf{1} & N \in \text{even} .\end{aligned}\quad (5.3.18)$$

Taking $q = 1$, the rhs of the above formulae reduce to

$$\frac{3^N - 1}{2} \begin{pmatrix} 1 & 1 \\ 1 & 1 \end{pmatrix}, \quad (5.3.19)$$

which is precisely the result derived in [7]. For arbitrary q , these formulae can be further simplified by noting that

$$\begin{aligned}(\mathbf{1} + \tilde{\mathbf{K}})(\mathbf{1} + \mathbf{K}) &= \frac{4}{(q+q^{-1})^2} (\mathbf{1} + (q^2 + q^{-2})(q + q^{-1})^2 \mathbf{P}) \\ (\mathbf{1} + \mathbf{K})(\mathbf{1} + \tilde{\mathbf{K}}) &= \frac{4}{(q+q^{-1})^2} (\mathbf{1} + (q^2 + q^{-2})(q + q^{-1})^2 \mathbf{P}')\end{aligned}\quad (5.3.20)$$

where

$$\mathbf{P} = \frac{1}{q + q^{-1}} \begin{pmatrix} q^{-1} & q^{-2} \\ q^2 & q \end{pmatrix}$$

and

$$\mathbf{P}' = \frac{1}{q + q^{-1}} \begin{pmatrix} q & q^{-2} \\ q^2 & q^{-1} \end{pmatrix}$$

satisfy the property

$$\mathbf{P}^{(\prime)2} = \mathbf{P}^{(\prime)}. \quad (5.3.21)$$

This relation, when combine with (5.3.14), gives the result of the contraction

$$\begin{aligned}(\Omega_{\gamma\delta}^{(N)}, \Omega_{\alpha\beta}^{(N)}) \left(\frac{q + q^{-1}}{2} \right)^N &= \frac{1}{q + q^{-1}} \begin{pmatrix} \Lambda^N - (-1)^N & q^{-1}\Lambda^N + (-1)^N q^{-3} \\ q\Lambda^N + (-1)^N q^3 & \Lambda^N - (-1)^N \end{pmatrix}_{\alpha\beta} \delta_{\alpha\gamma} \delta_{\beta\delta} \\ &\quad - (-1)^N \begin{pmatrix} 0 & 1 \\ 1 & 0 \end{pmatrix}_{\alpha\beta} \delta_{\alpha\delta} \delta_{\beta\gamma}\end{aligned}\quad (5.3.22)$$

where

$$\Lambda = q^2 + 1 + q^{-2}.$$

Again the $q = 1$ limit of this formula recovers the result of [7].

With this expression for the norm, the spin-spin correlation functions defined as

$$\langle S_i^\mu S_j^\nu \rangle_{\text{VBS}} = (\Omega_{\gamma\delta}^{(N)}, S_i^\mu S_j^\nu \Omega_{\alpha\beta}^{(N)}) / (\Omega_{\gamma\delta}^{(N)}, \Omega_{\alpha\beta}^{(N)}) \quad ; \mu, \nu \in \pm, z$$

in the VBS states can be computed by breaking down the numerator into

$$\begin{aligned}(\Omega_{\gamma\delta_{i-1}}^{(i-1)}, \Omega_{\alpha\beta_{i-1}}^{(i-1)}) \epsilon_{\delta_{i-1}\gamma_i} \epsilon_{\beta_{i-1}\alpha_i} (\psi_{\gamma_i\delta_i}, S_i^\mu \psi_{\alpha_i\beta_i}) \epsilon_{\delta_i\gamma_{i+1}} \epsilon_{\beta_i\alpha_{i+1}} (\Omega_{\gamma_{i+1}\delta_{j-1}}^{(j-i-1)}, \Omega_{\alpha_{i+1}\beta_{j-1}}^{(j-i-1)}) \epsilon_{\delta_{j-1}\gamma_j} \epsilon_{\beta_{j-1}\alpha_j} \\ (\psi_{\gamma_j\delta_j}, S_j^\nu \psi_{\alpha_j\beta_j}) \epsilon_{\delta_j\gamma_{j+1}} \epsilon_{\beta_j\alpha_{j+1}} (\Omega_{\gamma_{j+1}\delta}^{(N-j)}, \Omega_{\alpha_{j+1}\beta}^{(N-j)})\end{aligned}$$

and applying (5.3.22). We shall display only the result for the special case $\alpha = \gamma$ and $\beta = \delta$, where the nonvanishing correlation functions are

$$\begin{aligned}
\langle S_i^+ S_j^- \rangle_{11} &= (-1)^{j-1}(q+q^{-1})[a\Lambda^{N-j+i-1} - (-1)^i q^{-1} b\Lambda^{N-j} - (-1)^{N-j} q b\Lambda^{i-1} \\
&\quad + (-1)^{N-j+i} c]/(\Lambda^N - (-1)^N), \\
\langle S_i^+ S_j^- \rangle_{12} &= (-1)^{j-1}(q+q^{-1})[a\Lambda^{N-j+i-1} - (-1)^i q^{-1} b\Lambda^{N-j} + (-1)^{N-j} q^{-1} b\Lambda^{i-1} \\
&\quad - (-1)^{N-j+i} q^{-2} c]/(\Lambda^N + q^{-2}(-1)^N), \\
\langle S_i^+ S_j^- \rangle_{21} &= (-1)^{j-1}(q+q^{-1})[a\Lambda^{N-j+i-1} + (-1)^i q b\Lambda^{N-j} - (-1)^{N-j} q b\Lambda^{i-1} \\
&\quad - (-1)^{N-j+i} q^2 c]/(\Lambda^N + q^2(-1)^N), \\
\langle S_i^+ S_j^- \rangle_{22} &= (-1)^{j-1}(q+q^{-1})[a\Lambda^{N-j+i-1} + (-1)^i q b\Lambda^{N-j} + (-1)^{N-j} q^{-1} b\Lambda^{i-1} \\
&\quad + (-1)^{N-j+i} c]/(\Lambda^N - (-1)^N), \\
\langle S_i^- S_j^+ \rangle_{\alpha\beta} &= \langle S_i^+ S_j^- \rangle_{\alpha\beta}, \\
\langle S_i^z S_j^z \rangle_{\alpha\alpha} &= (-1)^{j-i}(q+q^{-1})^2 (\Lambda^{N-j+i-1} - (-1)^N \Lambda^{j-i}) / (\Lambda^N - (-1)^N), \\
\langle S_i^z S_j^z \rangle_{12} &= (-1)^{j-i}(q+q^{-1})^2 (q^{-2} \Lambda^{N-j+i-1} + (-1)^N \Lambda^{j-i}) / (\Lambda^N + q^{-2}(-1)^N), \\
\langle S_i^z S_j^z \rangle_{21} &= (-1)^{j-i}(q+q^{-1})^2 (q^2 \Lambda^{N-j+i-1} + (-1)^N \Lambda^{j-i}) / (\Lambda^N + q^2(-1)^N)
\end{aligned} \tag{5.3.23}$$

where

$$\begin{aligned}
a &= q^3 + 2 + q^{-3} \\
b &= q^2 - q + q^{-1} - q^{-2} \\
c &= q + q^{-1} - 2.
\end{aligned}$$

Before interpreting these formulae, we first examine the role of the VBS in the spectrum of the hamiltonian. For q real, one can extend the proof of the $q = 1$ case and show that the eigenvalues are always nonnegative, and VBS are the only ground states. In the infinite N limit, the ground state is unique with massive excitation. Hence, the model is noncritical with spin-spin correlation functions in the VBS given by

$$\begin{aligned}
\langle S_i^+ S_j^- \rangle &= \langle S_i^- S_j^+ \rangle \stackrel{N \rightarrow \infty}{\cong} (-\Lambda)^{-j+i} (q^3 + 2 + q^{-3}) / (q^2 + 1 + q^{-2}), \\
\langle S_i^z S_j^z \rangle &\stackrel{N \rightarrow \infty}{\cong} (-\Lambda)^{-j+i} (q^2 + 2 + q^{-2}) / (q^2 + 1 + q^{-2}).
\end{aligned} \tag{5.3.24}$$

The correlation length is therefore $1/\ln(q^2 + 1 + q^{-2})$ and notice that the nonisotropy of S_i^\pm and S_i^z in the hamiltonian (5.3.2) due to the quantum group symmetry is manifested in the above. Only when $q \rightarrow 1$ where $\text{su}(2)$ symmetry is present will isotropy in the spin components be restored.

Recall that the $q = 1$ model belongs to the more general antiferromagnetic fluid phase or disorder flat phase (DOF)[33]. It can likewise be demonstrated that for real q the VBS ground states have the type of long range order and disorder associated with DOF phase. The various correlation functions introduced in [33] that distinguish the DOF phase can be calculated. We list, in particular, the density-density correlation function

$$\langle (S_i^z)^2 (S_j^z)^2 \rangle_{\text{VBS}} \stackrel{N \rightarrow \infty}{\cong} \langle (S_i^z)^2 \rangle_{\text{VBS}} \langle (S_j^z)^2 \rangle_{\text{VBS}} \stackrel{N \rightarrow \infty}{\cong} \frac{4}{(q^2 + 1 + q^{-2})^2} \tag{5.3.25}$$

which confirms that spin positions are completely uncorrelated, and the correlation function which exhibits antiferromagnetic ordering,

$$G_s(j-i) = \langle S_i^z e^{(S_i^z + \dots + S_j^z)} S_j^z \rangle_{\text{VBS}} \stackrel{N \rightarrow \infty}{=} \frac{4}{(q^2 + 1 + q^{-2})^2} . \quad (5.3.26)$$

The lack of distance dependence shows that AF spin order is perfect.

For $q = e^{i\gamma}$, $\gamma \in \mathbf{R}$, the configuration space belongs to $(\mathbf{C}^3)^N$ and the reasoning that led to the proof of massive excitations for real q no longer holds. The eigenvalues can in fact be negative.

Numerical check reveals that for finite N the VBS continue to be the only ground state for $\gamma \in [0, \frac{\pi}{6})$ and $\gamma \in (\frac{2\pi}{5}, \frac{\pi}{2}]$. In the first domain, $q^2 + 1 + q^{-2} > 1$, so we expect the properties for real q to be still qualitatively valid, with massive excitations and a kind of DOF phase. The second domain has $|q^2 + 1 + q^{-2}| < 1$ so the behavior is now possibly different from the real q model, in particular, it is not sure whether excitations are still massive. For $\gamma \in (\frac{\pi}{6}, \frac{2\pi}{5})$, there are negative eigenenergies so we certainly expect different properties.

That another eigenenergy crosses the value zero at $\gamma = \frac{\pi}{6}$ can be shown using $U_q \text{su}(2)$ symmetry. Indeed the projector $(Q-1)(Q-2)P_2$ when restricted to type II representations satisfies the Temperley Lieb algebra with[17]

$$\begin{aligned} 2P_2 &= e_i \\ \text{and } e_i^2 &= 2e_i . \end{aligned} \quad (5.3.27)$$

The same algebra in the spin- $\frac{1}{2}$ representation given by

$$e_i = 2P_0 \quad (5.3.28)$$

with $2P_0$ acts on $\mathbf{C}^2 \otimes \mathbf{C}^2$ has "q" parameter of the quantum group given by "q" = 1 or ($\sqrt[{}]{q}$ = 2). The type II spectrum of $2P_2$ at $\gamma = \frac{\pi}{6}$ and the entire spectrum of $2P_0$ at "q" = 1 share the same set of eigenvalues. Moreover the q -dimensions (defined as $(2j+1)_q$) of the spin sectors from the two representations which share the same eigenvalues are equal. In particular, the zero eigenvalue, which occurs in the highest spin sector ($j = \frac{N}{2}$) of the spin- $\frac{1}{2}$ representation, has q -dimension

$$(2j+1)_1 = (N+1)_1 = N+1 ,$$

while in the spin-1 representation, the contribution to the q -dimension of the VBS states, which have $j = 0, 1$, amounts to

$$(2 \cdot 0 + 1)_q + (2 \cdot 1 + 1)_q = 1 + q^2 + 1 + q^{-2} = 3 < N+1 \quad ; \quad \text{for } N > 2$$

implying that new zero eigenvalues must emerge for spin chains with $N > 2$. As an example, at $N = 3$, we find a new zero eigenstate with $j = 2$, the q -dimension of which

$$(2 \cdot 2 + 1)_q = 1$$

adds to the above giving the total contribution

$$4(= N+1) .$$

The crossing of eigenvalues $\frac{2\pi}{5}$ (and also at $\frac{\pi}{5}$) can also be explained. The $j = 2$ spin representations are then type I representations and $(Q-1)(Q-2)P_2$ vanishes when restricted to type II representations. Thus all type II eigenvalues vanish.

Despite the fact that quantum group symmetry implies additional zero eigenstates have to emerge at $\frac{\pi}{6}$ and $\frac{2\pi}{5}$, we only have numerical support that this does not happen outside the domain $[\frac{\pi}{6}, \frac{2\pi}{5}]$.

We did not get definite numerical evidence for possible critical properties in the domain $[\frac{\pi}{6}, \frac{2\pi}{5}]$. Notice however the special value $\gamma = \frac{\pi}{3}$ where the P_2 projector line (5.3.1) meets the TL line, so there we have criticality with $c = -2$.

5.4 The Γ_2 Potts model

We have discussed the phase diagram of the quantum spin chain because it is the simplest and has most immediate applications. It is not always easy to discuss the relation of this study with the two dimensional Potts model. Clearly the above hamiltonians, although considered so far as acting on spins, can be rewritten as Potts hamiltonians using the appropriate representation of the projectors discussed earlier. It is reasonable to hope that the physics of these hamiltonians is the same as the one of a two dimensional strongly anisotropic Potts model whose elementary transfer matrix reads $1 + \epsilon H$. This correspondence is enough to apply to the quantum spin chain duality arguments deduced for a two dimensional (not necessarily isotropic) Potts model. However when couplings in two directions take comparable values, it is not clear whether the physics will or not be qualitatively different. This is especially true in our case where there are both ferromagnetic and antiferromagnetic interactions. In the integrable cases however, one can usually connect the physics for different isotropies by changing the spectral parameter, and exact solutions usually show that properties are the same provided this parameter runs in a certain range. Let us write the isotropic interactions associated with the three integrable lines discussed earlier (they will be recovered in the hamiltonian limit $u = 0$, $\epsilon = -1$. The case for $\epsilon = 1$ can similarly be studied.)

The Boltzmann weight associated to the fundamental block \mathcal{G}_2 has physical expression given by

$$W_{abcd} = \exp \mathcal{E}_{abcd} \quad (5.4.1)$$

where the interaction energy

$$\mathcal{E} = \mathcal{K}_0(Q-1)P_0 + \mathcal{K}_1(Q-1)P_1 .$$

Written in terms of the four sites a, \dots, d , the energy reads

$$\begin{aligned} \mathcal{E}_{abcd} = & (\mathcal{K}_0 - 4\mathcal{K}_1)Q^{-2} - (\mathcal{K}_0 - 2\mathcal{K}_1)Q^{-1}(\delta_{ab} + \delta_{cd}) + \mathcal{K}_1Q^{-1}(\delta_{ac} + \delta_{bd} + \delta_{ad} + \delta_{bc}) \\ & + (\mathcal{K}_0 - \mathcal{K}_1)\delta_{ab}\delta_{cd} - \mathcal{K}_1(\delta_{abc} + \delta_{abd} + \delta_{bcd} + \delta_{acd}) + \mathcal{K}_1Q\delta_{abcd} , \end{aligned} \quad (5.4.2)$$

which shows that the various interactions; nearest neighbors, next to nearest neighbors etc. can either be ferromagnetic or antiferromagnetic depending on the values of the coupling constants \mathcal{K}_0 and \mathcal{K}_1 . The dual model involves similar expressions.

The TL integrable line is given by

$$Q^{-1/2}f_1 = 0$$

which translates into

$$\begin{aligned} \mathcal{K}_0 &= \ln 2 / (Q-1) , \\ \text{and } \mathcal{K}_1 &= 0 . \end{aligned} \quad (5.4.3)$$

using (3.2.8) and $f_0 = 1$. In this case the energy expression becomes a product of $Q^{-1} - \delta_{ab}$ and $Q^{-1} - \delta_{cd}$ with \mathcal{K}_0 being the overall coefficient. The ferro- and antiferro-magnetic nature of the interactions therefore depend

only on the sign of \mathcal{K}_0 , which flips at $Q = 1$. For $Q > 1$ the model is characterized by antiferromagnetic nearest neighbors interaction and ferromagnetic four sites interaction $\delta_{ab}\delta_{cd}$, and the converse for $Q < 1$. It should be noted that the point $Q = 1$ corresponds to $Q' = 0$ of the Γ_1 (or standard) Potts model via the Temperley Lieb algebra. For the Γ_1 Potts model on the TL integrable line (3.6.7), $Q' = 0$ is precisely the point that divides the ferro- and anti-ferromagnetic regimes[6].

The FZ line is given by

$$Q^{-1/2}f_1 = \frac{1}{\sqrt{Q}+1}, \quad (5.4.4)$$

which is equivalent to

$$\begin{aligned} \mathcal{K}_0 &= \frac{\ln(Q + \sqrt{Q} - 1)}{Q - 1}, \\ \mathcal{K}_1 &= \frac{\ln(Q + \sqrt{Q} - 1) - \ln(\sqrt{Q} + 1)}{Q - 2} \end{aligned} \quad (5.4.5)$$

where the coupling constants at $Q = 1$ and $Q = 2$ are defined by continuity. It is easy to see that both \mathcal{K}_i 's are nonnegative functions of Q . However \mathcal{K}_0 becomes complex for $Q < (3 - \sqrt{5})/2$ (or $\gamma > 2\pi/5$) and the Potts model beyond that point is not physical. In the domain $Q > (3 - \sqrt{5})/2$, the magnetic nature of the interaction terms in the energy expression remain unchanged being always ferro- or antiferro-magnetic as the coefficients \mathcal{K}_1 , $\mathcal{K}_0 - \mathcal{K}_1$ and $\mathcal{K}_0 - 2\mathcal{K}_1$ are always positive.

The same analysis can be performed on the IK integrable line, which is given by

$$Q^{-1/2}f_1 = -1 + \sqrt{4 - Q} \quad (5.4.6)$$

or equivalently

$$\begin{aligned} \mathcal{K}_0 &= \frac{\ln(1 + (Q - 1)\sqrt{4 - Q})}{Q - 1}, \\ \mathcal{K}_1 &= \frac{\ln(3 - Q + (Q - 2)\sqrt{4 - Q})}{Q - 2}. \end{aligned} \quad (5.4.7)$$

The coupling constants are real for $Q \in (0.77, 3.80)$ approximately. As Q increases from 0.77 in this domain, the majority of the interaction terms which have coefficient proportional to \mathcal{K}_1 changes from ferromagnetic to antiferromagnetic or vice versa at $Q = 3$. In the phase diagram this is the point that divides the various regimes of the integrable line. Since $\mathcal{K}_1 > 0$ as in the FZ case, the magnetic natures of the majority of the interactions of the IK integrable model for $Q < 3$ are the same as that of the FZ integrable model. The exception being the interactions $\delta_{ab}\delta_{cd}$ and $\delta_{ab} + \delta_{cd}$, whose respective coefficients $\mathcal{K}_0 - \mathcal{K}_1$ and $\mathcal{K}_0 - 2\mathcal{K}_1$ change from negative to positive at $Q \simeq 0.8$ and $Q \simeq 1.9$. This similarity in the physical behaviors of the interactions supports the conclusion reached in the spin chain study that the two lines are in the same universality for $Q < 3$.

6 Conclusion

Γ_k Potts models provide a rather different kind of physical models associated with spin- $k/2$ representations of $U_q\text{su}(2)$, where the higher symmetry constraints are encoded in a pattern of complicated interactions on a plaquette. Besides their "academic" interest we hope they can provide new insight on the physics of related solutions of Yang Baxter equation, or universality classes. For instance the standard $\text{su}(2)$ symmetric

quantum spin chains are related to $Q = 4$ states Potts models with a mixture of ferromagnetic and antiferromagnetic interactions. The splitting between integer and half integer spin is very naturally observed in this picture. A translation invariant quantum spin chain is the anisotropic limit of a four state Potts model based on a homogeneous vertex model. For half integer spin (k odd) this Potts model turns out to be necessarily self dual. One therefore expect it, by standard arguments, to be at a critical point. On the other hand for integer spin (k even) the Potts model is not self dual, and generically is expected to be in some non critical state. This is quite close to the Haldane conjecture.

The technology of quantum groups, Temperley Lieb algebras and graphical representations is known under other names in the condensed matter literature[47]. In particular it was remarked in [47] that the standard Q state Potts model can be related to a quantum spin chain with $su(n)$ symmetry, with the fundamental representation on a sub lattice and its conjugate on the other, and $n = \sqrt{Q}$. More generally one can speculate that systems with quantum group symmetries provide proper analytic continuations of models with ordinary symmetries when the rank of the algebra or the size of the representation assume "intermediate" values. For instance the spin 1 $U_q su(2)$ model, or equivalently the Γ_2 Potts model, can be related to a quantum spin chain with $su(n)$ symmetry, once again $n = \sqrt{Q}$, but with the adjoint representation on every site. This is because $(3)_q = n^2 - 1$. As shown in section 5 of this paper, the phase diagram is rich. In particular several critical lines and massless phases are met in the continuation from $n = 2$ ($q = 1$) to $n = 0$ ($q = i$), which is of interest for the quantum Hall effect [47]. As the representation gets more complex we expect this continuation to "go through" a more and more complicated phase diagram.

Finally we remark that the quantum group symmetric models are also a particular example of anisotropic quantum spin chains. From that point of view, the last paragraph in section 5 represents an extension of the valence bond method to a particular anisotropic situation.

Acknowledgments: I. Affleck, B.Nienhuis and N.Read are thanked for useful discussions.

A Boltzmann Factor of Γ_3 Potts model

The Boltzmann weight of the Γ_3 Potts model contains interactions between all the six sites a, \dots, f , the explicit form is given by

$$\begin{aligned}
W(u)_{aebcfd} = & (Q-1)^{-2} \{ \delta_{ef} - (Q-1)\delta_{ef}(\delta_{bd} + \delta_{ac}) - (\delta_{efa} + \delta_{efb} + \delta_{efc} + \delta_{efd}) + \delta_{abef} + \delta_{adef} \\
& + \delta_{bcef} + \delta_{cdef} + Q(\delta_{bdef} + \delta_{acef}) + (Q-1)(\delta_{bd}\delta_{aef} + \delta_{bd}\delta_{cef} + \delta_{ac}\delta_{bef} + \delta_{ac}\delta_{def}) \\
& - Q(\delta_{abdef} + \delta_{acdef} + \delta_{abcef} + \delta_{bcdef}) - Q(Q-1)(\delta_{ac}\delta_{bdef} + \delta_{bd}\delta_{acef}) \\
& + (Q-1)^2\delta_{ac}\delta_{bd}\delta_{ef} + Q^2\delta_{abcdef} \} \\
& + Q^{-1/2}h(Q-1)^{-2} \{ 1 - (\delta_{cf} + \delta_{fd} + \delta_{be} + \delta_{ae}) - (Q-1)(\delta_{ab} + \delta_{cd}) + Q(\delta_{abe} + \delta_{cdf}) \\
& + \delta_{ae}\delta_{cf} + \delta_{ae}\delta_{df} + \delta_{be}\delta_{cf} + \delta_{be}\delta_{df} + (Q-1)(\delta_{be}\delta_{cd} + \delta_{ae}\delta_{cd} + \delta_{ab}\delta_{cf} + \delta_{ab}\delta_{df}) \\
& + (Q-1)^2\delta_{ab}\delta_{cd} - Q(\delta_{ae}\delta_{cfd} + \delta_{be}\delta_{cfd} + \delta_{cf}\delta_{abe} + \delta_{df}\delta_{abe}) - Q(Q-1)(\delta_{ab}\delta_{cdf} + \delta_{cd}\delta_{abe}) \\
& + Q^2\delta_{abe}\delta_{cdf} \} \\
& + f(Q-1)^{-4} \{ 2 - 3Q + (3Q-2)(\delta_{be} + \delta_{cf} + \delta_{df} + \delta_{ae}) + (Q-1)(\delta_{bf} + \delta_{de} + \delta_{ce} + \delta_{af}) \\
& + \delta_{ef} + (Q-1)^2(\delta_{bd} + \delta_{cd} + \delta_{bc} + \delta_{ad} + \delta_{ab} + \delta_{ac}) - Q(\delta_{bef} + \delta_{def} + \delta_{aef} + \delta_{cef}) \\
& - (Q-1)^2(\delta_{cde} + \delta_{abf}) - Q(Q-1)(\delta_{bde} + \delta_{bdf} + \delta_{bcf} + \delta_{ade} + \delta_{bce} + \delta_{adf} + \delta_{acf} + \delta_{ace}) \\
& + (1-Q-Q^2)(\delta_{cfd} + \delta_{abe}) - (Q-1)^3(\delta_{bcd} + \delta_{abd} + \delta_{abc} + \delta_{acd}) + (2-3Q)(\delta_{be}\delta_{cf} \\
& + \delta_{be}\delta_{df} + \delta_{ae}\delta_{df} + \delta_{ae}\delta_{cf}) - (Q-1)(\delta_{de}\delta_{cf} + \delta_{ae}\delta_{bf} + \delta_{df}\delta_{ec} + \delta_{be}\delta_{af}) \\
& - (Q-1)^2(\delta_{bd}\delta_{cf} + \delta_{be}\delta_{cd} + \delta_{bc}\delta_{df} + \delta_{ae}\delta_{cd} + \delta_{bc}\delta_{ae} + \delta_{ad}\delta_{be} + \delta_{ab}\delta_{df} + \delta_{ad}\delta_{cf} + \delta_{ac}\delta_{be} \\
& + \delta_{ac}\delta_{df} + \delta_{ab}\delta_{fc} + \delta_{bd}\delta_{ae}) + Q^2(\delta_{bdef} + \delta_{acef} + \delta_{bcef} + \delta_{cdef} + \delta_{abef} + \delta_{adef}) \\
& + Q(Q-1)^2(\delta_{bcde} + \delta_{acde} + \delta_{abdf} + \delta_{abcf}) + Q^2(Q-1)(\delta_{abce} + \delta_{abde} + \delta_{bcdf} + \delta_{acdf}) \\
& + (Q^2 + Q-1)(\delta_{cdf}\delta_{be} + \delta_{cdf}\delta_{ae} + \delta_{abe}\delta_{df} + \delta_{abe}\delta_{cf}) + Q(Q-1)(\delta_{bde}\delta_{cf} + \delta_{bdf}\delta_{ae} \\
& + \delta_{acf}\delta_{be} + \delta_{ace}\delta_{df} + \delta_{ade}\delta_{cf} + \delta_{bcf}\delta_{ae} + \delta_{bce}\delta_{df} + \delta_{adf}\delta_{be}) + (Q-1)^2(\delta_{abe}\delta_{cd} + \delta_{cdf}\delta_{ab}) \\
& + \delta_{abcd} + (Q-1)^3(\delta_{abc}\delta_{df} + \delta_{acd}\delta_{be} + \delta_{dcb}\delta_{ae} + \delta_{abd}\delta_{fc}) \\
& - Q^3(\delta_{bcdef} + \delta_{abdef} + \delta_{abcef} + \delta_{acdef}) - Q^2(Q-1)^2(\delta_{abcde} + \delta_{abcdf}) - Q(2Q-1)\delta_{abe}\delta_{cdf} \\
& + (Q-1)^2(\delta_{bd}\delta_{fc}\delta_{ae} + \delta_{bc}\delta_{fd}\delta_{ae} + \delta_{ad}\delta_{be}\delta_{fc} + \delta_{ac}\delta_{be}\delta_{fd}) + Q^4\delta_{abcdef} \\
& - Q^2(Q-1)(\delta_{abde}\delta_{cf} + \delta_{bcdf}\delta_{ae} + \delta_{abce}\delta_{df} + \delta_{acdf}\delta_{be}) \} \\
& + Q^{-1/2}g(Q-1)^{-4} \{ Q^2 + (1-2Q)\delta_{ef} - Q(Q-1)^2(\delta_{ac} + \delta_{bd}) - Q^2(\delta_{ae} + \delta_{be} + \delta_{cf} + \delta_{df}) \\
& - Q(Q-1)(\delta_{ed} + \delta_{ec} + \delta_{bf} + \delta_{af}) + (Q^2 + Q-1)(\delta_{efd} + \delta_{efb} + \delta_{efc} + \delta_{efa}) + Q^2(\delta_{cfd} + \delta_{abe}) \\
& + Q(Q-1)(\delta_{bfc} + \delta_{bec} + \delta_{adf} + \delta_{ade}) + Q^2(Q-1)(\delta_{bed} + \delta_{bfd} + \delta_{acf} + \delta_{ace}) \\
& + (Q-1)^2(\delta_{afb} + \delta_{cde} + \delta_{ac}\delta_{ef} + \delta_{bd}\delta_{ef}) + Q(Q-1)^2(\delta_{bd}\delta_{fc} + \delta_{bd}\delta_{ae} + \delta_{be}\delta_{ac} + \delta_{ac}\delta_{df}) \\
& + Q^2(\delta_{be}\delta_{fc} + \delta_{ae}\delta_{fd} + \delta_{ae}\delta_{fc} + \delta_{be}\delta_{df}) + (Q-1)^3(\delta_{af}\delta_{bd} + \delta_{ec}\delta_{bd} + \delta_{ac}\delta_{bf} + \delta_{ac}\delta_{de}) \\
& + Q(Q-1)(\delta_{ec}\delta_{fd} + \delta_{af}\delta_{be} + \delta_{ae}\delta_{bf} + \delta_{cf}\delta_{ed}) + (Q-1)^2(\delta_{bf}\delta_{ec} + \delta_{af}\delta_{ed}) \\
& + (Q-1)^4\delta_{ac}\delta_{bd} + Q(1-Q-Q^2)(\delta_{acef} + \delta_{bdef}) + Q(2-3Q)(\delta_{cdef} + \delta_{abef} + \delta_{bcef} + \delta_{adef}) \\
& - Q^2(Q-1)(\delta_{acdf} + \delta_{bcdf} + \delta_{abde} + \delta_{abce}) - Q(Q-1)^2(\delta_{bcde} + \delta_{acde} + \delta_{abcf} + \delta_{abdf}) \\
& - Q^2(\delta_{be}\delta_{cfd} + \delta_{ae}\delta_{cfd} + \delta_{abe}\delta_{cf} + \delta_{abe}\delta_{df}) - Q^2(Q-1)(\delta_{bde}\delta_{fc} + \delta_{acf}\delta_{be} + \delta_{ace}\delta_{fd} + \delta_{bdf}\delta_{ae})
\end{aligned}$$

$$\begin{aligned}
& - Q(Q-1)^2(\delta_{ace}\delta_{bf} + \delta_{bdf}\delta_{ec} + \delta_{efc}\delta_{bd} + \delta_{bde}\delta_{af} + \delta_{bef}\delta_{ac} + \delta_{efd}\delta_{ac} + \delta_{afc}\delta_{ed} + \delta_{aef}\delta_{bd}) \\
& - Q(Q-1)(\delta_{bec}\delta_{fd} + \delta_{adf}\delta_{be} + \delta_{aed}\delta_{fc} + \delta_{bcf}\delta_{ae}) + Q^2\delta_{abe}\delta_{cdf} + Q^2(2-3Q)\delta_{abcdef} \\
& - Q(Q-1)^3(\delta_{bde}\delta_{ac} + \delta_{bdf}\delta_{ac} + \delta_{acf}\delta_{bd} + \delta_{ace}\delta_{bd}) + Q^2(3Q-2)(\delta_{abcef} + \delta_{abdef} + \delta_{bcdef} \\
& + \delta_{acdef}) + Q^2(Q-1)^2(\delta_{abcdf} + \delta{abcde} + \delta_{bdef}\delta_{ac} + \delta_{acef}\delta_{bd} + \delta_{afc}\delta_{bde} + \delta_{ace}\delta_{bdf}) \\
& - Q(Q-1)^2(\delta_{ac}\delta_{be}\delta_{df} + \delta_{bd}\delta_{ae}\delta_{cf}) + Q^2(Q-1)(\delta_{acdf}\delta_{be} + \delta_{bcdaf}\delta_{ae} + \delta_{abde}\delta_{cf} + \delta_{abce}\delta_{df})\}
\end{aligned}$$

B Loop Model Formulation of the Γ_k model

We present in this appendix a brief review of the known loop model formulations of the Γ_k model.

B.1

First we recall the standard graphical representation of the Temperley-Lieb algebra[50, 51] with the representation space being a set of strands. The generator e_i acts on two neighboring strands and produces the following configurations

$$e_i \quad \begin{array}{c} \text{---} \\ \text{---} \end{array} \longrightarrow \begin{array}{c} \diagup \quad \diagdown \\ \diagdown \quad \diagup \end{array}$$

while the identity leaves the strands unaltered

$$\mathbf{1} \quad \begin{array}{c} \text{---} \\ \text{---} \end{array} \longrightarrow \begin{array}{c} \diagdown \quad \diagup \\ \diagup \quad \diagdown \end{array}$$

With this definition, the algebraic relations (2.6) are represented as

$$\begin{array}{c} \diagup \quad \diagdown \quad \diagup \quad \diagdown \\ \diagdown \quad \diagup \quad \diagdown \quad \diagup \end{array} \longrightarrow \begin{array}{c} \diagup \quad \diagdown \\ \text{---} \end{array}$$

$$e_i e_{i+1} e_i = e_i$$

and

$$\begin{array}{c} \diagup \quad \diagdown \\ \diagdown \quad \diagup \end{array} \longrightarrow \sqrt{Q} \begin{array}{c} \diagup \quad \diagdown \\ \diagdown \quad \diagup \end{array}$$

$$e_i^2 = \sqrt{Q} e_i$$

which are easily seen to be satisfied in this representation provided every loop is given a weight \sqrt{Q} . Such a reformulation was rediscovered many times, in particular in [47] using valence bond language.

This gives a geometrical reformulation of the six-vertex model (known also as loop model formulation) where the vertex $x_1 \mathbf{1} + e_{2i-1}$ or $\mathbf{1} + x_2 e_{2i}$ are replaced by the graphical combinations

$$x_1 \begin{array}{c} \diagup \\ \diagdown \end{array} + \begin{array}{c} \diagdown \\ \diagup \end{array} \quad \text{or} \quad \begin{array}{c} \diagdown \\ \diagup \end{array} + x_2 \begin{array}{c} \diagup \\ \diagdown \end{array}$$

and the lattice is accordingly covered by a collection of closed loops. From the Potts model point of view, these are the surrounding polygons of clusters high temperature expansion.

Recall that there are some subtleties about the models correspondence due to boundary conditions.

Using the fusion procedure, a loop model formulation can be given to the Γ_k vertex model [52, 51, 15]. Graphically, this is done by replacing each of the six-vertex in (3.1.4) by one of the above configurations. Each spin- $\frac{k}{2}$ vertex therefore acts on $2k$ strands, the symmetrizer S_k that acts on k strands is represented by

$$S_k \quad \begin{array}{c} \text{---} \\ \text{---} \\ | \\ \vdots \\ | \\ \text{---} \\ \text{---} \end{array}$$

Figure(B0) The composite k -strand that denotes the symmetrizer S_k

which is a composite object given by (3.1.3). As an example for $k = 2$

$$S_2 = \mathbf{1} - \frac{1}{(2)_q} e$$

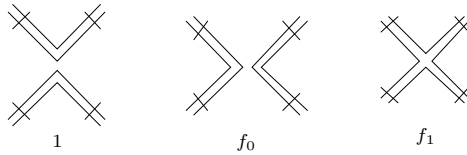
has graphical representation

$$S_2 \quad \equiv \quad \begin{array}{c} \text{---} \\ \text{---} \\ | \\ | \end{array} = \begin{array}{c} \diagdown \\ \diagup \end{array} - \frac{1}{(2)_q} \begin{array}{c} \diagdown \\ \diagup \end{array}$$

The internal vertices $r_k(u_1), \dots, r_k(u_{k^2})$ that are inserted between the four copies of S_k represented above produce in general 2^{k^2} configurations. However, configurations that have any two strands that originate from the same symmetrizer joined together have vanishing weight, since this implies the presence of the factor

$$P_1 P_0 = 0$$

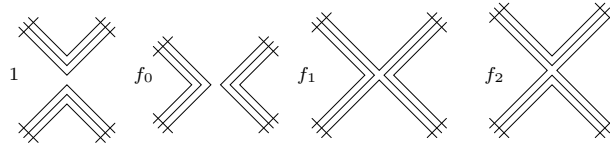
where P_1 comes from the symmetrizer and $P_0 \propto e$ from the fusing of the two strands. Hence for $k = 2$, the nonvanishing configurations are those shown in fig.(B1).



Figure(B1) The nonvanishing strand configurations of the loop model formulation of the Γ_2 model

In general, the Γ_k vertex is replaced by $k + 1$ nonvanishing strands configurations. (For $k = 3$, see fig.(B2)) These strands are again the surrounding polygons of the fused Potts models introduced earlier. In this fused loop model, a closed composite k -strand obtained by fusing the individual strands in fig.(B0) into loops carries a weight $(k + 1)_q$.

In such a formulation the numbers of degrees of freedom at each vertex is vastly reduced, but one has instead to deal with nonlocal quantities.



Figure(B2) Nonvanishing strand configurations for the Γ_3 model

B.2

For $k = 2$, there exist other loop model formulations. The first is due to the observation that[48]

$$\begin{aligned} b_i &= q^{-2} - (q^2 + q^{-2})P_1(i, i + 1) + q(q^3 - q^{-3})P_0(i, i + 1) , \\ e_i &= (q^2 + 1 + q^{-2})P_0(i, i + 1) \end{aligned} \quad (\text{B.2.1})$$

satisfy the Birman Wenzl Murakami (BWM) algebra[49]. The latter contains the Temperley-Lieb algebra generated by e_i with $\sqrt{m}Q^m = q^2 + 1 + q^{-2}$ as a subalgebra, and b_i satisfies the braid group relation

$$b_i b_{i\pm 1} b_i = b_{i\pm 1} b_i b_{i\pm 1} . \quad (\text{B.2.2})$$

They have graphical representations defined by the action on two neighboring strands;

$$\begin{aligned} \mathbf{1} : & \quad \longrightarrow \quad \begin{array}{c} \diagup \\ \diagdown \end{array} \\ b_i : & \quad \longrightarrow \quad \begin{array}{c} \diagdown \\ \diagup \end{array} \\ e_i : & \quad \longrightarrow \quad \begin{array}{c} \diagdown \quad \diagup \\ \diagup \quad \diagdown \end{array} \end{aligned}$$

Besides the Temperley Lieb and braid group relations, these generators satisfy some other algebraic relations which can be represented graphically. Most of these relations are then straightforwardly expressed by regular isotopy of the diagrams. The others are :

1.) The first Reidemester move

$$\begin{array}{c} \diagdown \\ \diagup \end{array} \begin{array}{c} \diagup \\ \diagdown \end{array} = q^4 \begin{array}{c} \diagdown \\ \diagup \end{array}$$

produces a factor q^4 .

2.) The relation $b_i - b_i^{-1} = (q^{-2} - q^2)(\mathbf{1} - e_1)$ holds, which can be represented graphically as

$$\begin{array}{c} \diagup \diagdown \\ \diagdown \diagup \end{array} - \begin{array}{c} \diagdown \diagup \\ \diagup \diagdown \end{array} = q^{-2} - q^2 \left(\begin{array}{c} \diagdown \diagup \\ \diagup \diagdown \end{array} - \begin{array}{c} \diagup \diagdown \\ \diagdown \diagup \end{array} \right)$$

3.) A loop carries a weight $(3)_q$.

$$\diamond = (3)_q$$

In terms of these generators, the vertex given in (3.2.1) is written as

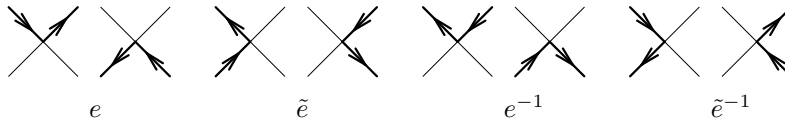
$$1 + q^{-2}\bar{f}_1 + (f_0 + q^2\bar{f}_1)e_i - \bar{f}_1 b_i \tag{B.2.3}$$

where

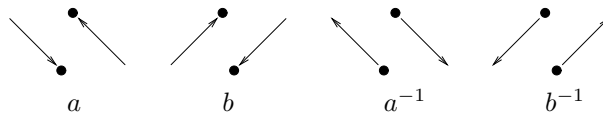
$$\bar{f}_1 = f_1/\sqrt{Q}.$$

B.3

The two above mappings have the drawback that they involve dense loop coverings of the lattice. An elegant way of mapping the Γ_2 model to a "dilute" loop model is given in [4]. In a first step one uses the edges of the vertices that carry the states $|\pm\rangle$ to form oriented loops, whose direction is given by the spin arrows, while edges with the state $|0\rangle$ are regarded as unoccupied. This gives an oriented dilute loop reformulation. The problem then is to find under what circumstances one can get rid of the orientations. The simplest way to find a correspondence between an oriented and an unoriented loop model is to suppose that in the unoriented model loops have a fugacity. This fugacity can be obtained by a sum of local contributions if one gives arbitrary orientations to the loops and sums over all possible orientations, provided a phase factor $e^{\pm 1}$ or $\tilde{e}^{\pm 1}$ has been assigned to every turn as follows

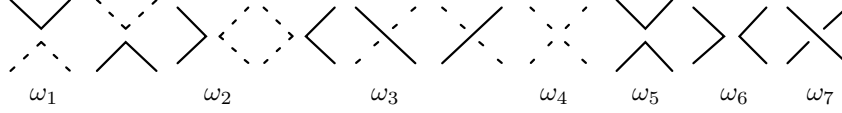


For a lattice which has the geometry of a plane, a closed loop has weight $e^2\tilde{e}^2(e^{-2}\tilde{e}^{-2})$ if the orientation is anticlockwise(clockwise)and so gets fugacity (weight) n equal to $e^2\tilde{e}^2 + e^{-2}\tilde{e}^{-2}$. In addition, to every edge of the vertex, one can assign, without altering the partition function, a local phase factor as follows



where the solid dot denotes the center of the vertex.

In an unoriented model, one has the following local loop configurations



where solid (dotted) strand denotes occupied (unoccupied) edge and ω_i 's, and for the last configuration the way the two strands overlap has no significance. If moreover the loops have fugacity n it is then equivalent to an oriented loop model, that is to a 19 vertex model, with weights which are products of ω_i and a, b, e, \tilde{e}

$$\begin{aligned}
V_{00,00} &= \omega_4, \\
V_{+0,+0} &= V_{0-,0-} = \omega_1 e a b^{-1}, \\
V_{0+,0+} &= V_{-0,-0} = \omega_1 e^{-1} a^{-1} b, \\
V_{+-,00} &= V_{00,+} = \omega_2 \tilde{e}^{-1} a b^{-1}, \\
V_{-+,00} &= V_{00,-} = \omega_2 \tilde{e} a^{-1} b, \\
V_{+,+,+} &= V_{-,-,-} = \omega_5 + \omega_7, \\
V_{+,-,-} &= V_{-+,+} = \omega_6 + \omega_7, \\
V_{+,-,+} &= \omega_6 \tilde{e}^{-2} a^2 b^{-2} + \omega_5 e^2 a^2 b^{-2}, \\
V_{-+,-} &= \omega_6 \tilde{e}^2 a^{-2} b^2 + \omega_5 e^{-2} a^{-2} b^{-2}, \\
V_{+0,0+} &= V_{0+,+0} = V_{0-,0-} = V_{-0,-0} = \omega_3
\end{aligned} \tag{B.3.1}$$

where $V_{ij,kl}$ denotes the vertex weight with in- and out- states being ij and kl respectively.

We thus see that the natural oriented loop model associated with the 19 vertex model is equivalent to an unoriented one provided the weights can be parametrized as above. This gives rise to a necessary condition

$$\frac{\frac{V_{+0,+0}}{V_{0+,+0}} + \frac{V_{+-,00}}{V_{-+,00}}}{\frac{V_{0+,+0}}{V_{+0,+0}} + \frac{V_{-+,00}}{V_{+-,00}}} = \frac{(V_{+,-,-} - V_{+,+,+}) \frac{V_{+0,+0}}{V_{0+,+0}} + V_{+,-,+}}{(V_{+,-,-} - V_{+,+,+}) \frac{V_{0+,+0}}{V_{+0,+0}} + V_{-+,-}}. \tag{B.3.2}$$

This holds in particular for the Γ_2 vertex model (ie when the 19 vertex model has $U_q \mathfrak{su}(2)$, for which the correspondence between the parameters $\omega_i, a, b, e, \tilde{e}$ and f_0, \bar{f}_1 is given by

$$\begin{aligned}
\omega_1 &= (1 + q^{-2} \bar{f}_1)^{1/2} (1 + q^2 \bar{f}_1)^{1/2}, \\
\omega_2 &= (f_0 + q^{-2} \bar{f}_1)^{1/2} (f_0 + q^2 \bar{f}_1)^{1/2}, \\
\omega_3 &= -\bar{f}_1, \\
\omega_4 &= 1 + f_0 + (Q - 3) \bar{f}_1, \\
\omega_5 &= \frac{(1 + q^2 \bar{f}_1)(1 + q^{-2} \bar{f}_1)(f_0 + \bar{f}_1)}{f_0 + f_1 + f_0 f_1 + (Q - 3) f_1^2}, \\
\omega_6 &= \frac{(f_0 + q^2 \bar{f}_1)(f_0 + q^{-2} \bar{f}_1)(1 + \bar{f}_1)}{f_0 + f_1 + f_0 f_1 + (Q - 3) f_1^2}, \\
\omega_7 &= -\frac{\bar{f}_1^2 + (Q - 3) f_0 \bar{f}_1 + f_0 \bar{f}_1^2 + \bar{f}_1^3}{f_0 + f_1 + f_0 f_1 + (Q - 3) f_1^2}
\end{aligned} \tag{B.3.3}$$

and the loop fugacity reads

$$n = q^2 \frac{(1 + q^{-2} \bar{f}_1)(f_0 + q^{-2} \bar{f}_1)}{(1 + q^2 \bar{f}_1)(f_0 + q^2 \bar{f}_1)} + q^{-2} \frac{(1 + q^2 \bar{f}_1)(f_0 + q^2 \bar{f}_1)}{(1 + q^{-2} \bar{f}_1)(f_0 + q^{-2} \bar{f}_1)}. \tag{B.3.4}$$

In this loop reformulation there are more degrees of freedom at each vertex than in the first one we discussed. Not all edges are occupied. The fugacity depends on f_0 and f_1 .

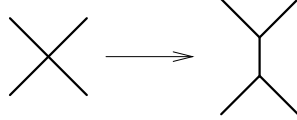
Consider now the case

$$\bar{f}_1 = -1, \quad f_0 = 0. \quad (\text{B.3.5})$$

The nonvanishing weights after rescaling become

$$\text{and} \quad \begin{aligned} \omega_2 &= \omega_3 = \omega_5 = 1, \\ \omega_1^2 &= \omega_4 = -(q - q^{-1})^2, \end{aligned} \quad (\text{B.3.6})$$

the vanishing of ω_5 and ω_7 implies that, if vertices are "expanded" as



such that the entire lattice becomes honeycomb, every edge can at most be occupied by one strand. Moreover, since the nonvanishing weights satisfy the relations given above, the model belongs to a subset of the class of loop model where loops do not intersect and the only parameters are loop and vacant site fugacities[53] $\{n, \omega_1\}$. In this case, the two parameters are related as

$$n = 2 - (2 - \omega_1^2)^2. \quad (\text{B.3.7})$$

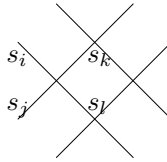
The integrable lines IK, TL and FZ play distinctive roles here too, they arise as a result of the restriction

- IK, TL : $\omega_7 = 0$
- FZ : vertex weights being invariant under reversal of all arrows and $n=2$.

For general f_0, \bar{f}_1 , the loops can be interpreted as high temperature expansion of an $O(n)$ model which has Boltzman weight

$$\begin{aligned} &\omega_4 + \omega_1(\vec{s}_i \cdot \vec{s}_k + \vec{s}_j \cdot \vec{s}_l) + \omega_2(\vec{s}_i \cdot \vec{s}_j + \vec{s}_k \cdot \vec{s}_l) + \omega_3(\vec{s}_i \cdot \vec{s}_l + \vec{s}_j \cdot \vec{s}_k) \\ &\omega_5(\vec{s}_i \cdot \vec{s}_j)(\vec{s}_k \cdot \vec{s}_l) + \omega_6(\vec{s}_i \cdot \vec{s}_k)(\vec{s}_j \cdot \vec{s}_l) + \omega_7(\vec{s}_i \cdot \vec{s}_l)(\vec{s}_j \cdot \vec{s}_k) \end{aligned}$$

where \vec{s}_i 's are n -component vectors situated on the edges of each vertex and are normalized as $\vec{s}_i \cdot \vec{s}_i = n$.



References

- [1] Baxter,R.J.:*Exactly Solved Models in Statistical Mechanics*, New York, (Academic Press)1982, Wu,F.Y.:*Rev. Mod. Phys.*, **54**, 235(1982).
- [2] Akutsu,Y., Kuniba,A. and Wadati,M.:*J.Phys. Soc. Jap.*, **9**, 2907(1986).
- [3] Lieb,E.H.:*Phys. Rev.*, **162**, 162(1967).
- [4] Nienhuis,B.:*Int. J. Mod. Phys.*, **B4**, 929(1990).
- [5] Kulish,P.P., Reshetikhin,N.Yu and Sklyanin,E.K.: *Lett. Math. Phys.*, **5**, 393 (1981), Jimbo,M.,Miwa,T. and Okado,M.:*Lett. Math. Phys.*, **14**, 123(1987).
- [6] Saleur,H.:*Commun. Math. Phys.*, **132**, 657(1990).
Saleur,H.:*Nucl.Phys.*, **B360**, 219(1991).
- [7] Affleck,I., Kennedy,T., Lieb,E.H. and Tasaki,H.:*Commun. Math. Phys.*, **115**, 477(1988).
- [8] Temperley,H.N.V. and Lieb,E.H.:*Pro. Roy. Soc.*, London, **A322**, 251(1971).
- [9] Jones,V.:*Invent.Math.*, **72**, 1(1983).
- [10] Drinfeld,V.G.:*dokl. Akad. Nank.*, SSSR **283**, 1060(1985),
Jimbo,M.:*Lett. Math. Phys.*, **10**, 63(1985),
Drinfeld,V.G.:Pro. ICM (AMS Berkeley) 1978 and references therein.
- [11] Pasquier,V. and Saleur,H.:*Nucl. Phys.*, **B330**, 523(1990).
- [12] Saleur,H. and Zuber,J.-B.:Proc. of Trieste Spring School, (1990).
- [13] di Francesco,P., Saleur,H. and Zuber,J.-B.:*Nucl. Phys.*, *B300*, 393(1988).
- [14] Jimbo,M.:*Lett. Math. Phys.*, **11**, 247(1986).
- [15] Saleur,H.:”*Geometrical Lattice Models for N=2 supersymmetric Theories in Two Dimensions*”, preprint YCTP-P39-91.
- [16] Izergin,A.G. and Korepin,V.E.:*Commun. Math. Phys.*, **79**, 303(1981).
- [17] Saleur,H. and Altschuler, D.:*Nucl. Phys.*, **B354**, 579(1991).
- [18] Wenzl,H.:*Invent. Math.*, **92**, 349(1988).
- [19] Syozi,I.:”*Phase transition and critical phenomena*”, **Vol 1**, Domb,C. and Green,M.S., Academic Press(1972).
- [20] Baxter,R.J.:*J. Phys. A*, **15**, 3329(1982).
- [21] Kelland,S.B.:*Can. J. Phys.*, **54**, 1621(1976).

- [22] Beijeren, V.: *Phys. Rev. Lett.*, **38**, 993(1977).
- [23] Andrews, G.E., Baxter, R.J. and Forrester, P.J.: *J. Stat. Phys.*, **35**, 193(1984).
- [24] Date, E., Jimbo, M., Kuniba, A., Miwa, T. and Okado, M.: *Nucl. Phys.*, **B290**[**FS20**], 231(1987).
- [25] Forrester, P.J.: *J. Phys. A*, **19**, L143(1986).
- [26] Saleur, H.: *J. Phys. A*, **22**, L41(1988).
- [27] Kac, V.G. and Peterson, D.: *Adv. Math.*, **53**, 125(1984).
- [28] Jimbo, M, Miwa, T. and Okado, M.: *Nucl. Phys.*, **B275**[**FS17**], 517(1986).
- [29] Cardy, J.L., Nauenberg, M. and Scalapino, D.J.: *Phys. Rev.*, **B22**, 2560(1980).
- [30] Affleck, I.: *Nucl. Phys.*, **B265**[**FS15**], 409(1986),
Barber, M.N. and Batchelor, M.T.: *Phys. Rev. B* **40** 4621(1989),
Papanicolaou, N.: *Nucl. Phys.* **B305**[**FS23**] 367(1988).
- [31] Lai, C.K.: *J. Math. Phys.*, **15**, 1675(1974),
Sutherland, B.: *Phys. Rev. B* **12**, 3795(1975),
Uimin, G.V.: *JETP Lett.* **12**, 225(1970).
- [32] Takhtajan, L.A.: *Phys. Lett. A*, **87**, 479(1982),
Babujian, H.M.: *Nucl. Phys.* **B215**, 317(1983).
- [33] den Nijs, M. and Rommelse, K.: *Phys. Rev. B*, **40**, 4709 (1989).
- [34] Jimbo, M.: *Commun. Math. Phys.*, **102**, 537(1986).
- [35] Zamolodchikov, A.B. and Fateev, V.A.: *Sov. J. Phys.*, **32**, 298(1980).
- [36] Batchelor, M., Mezincescu, L., Nepomechie, R.I. and Rittenberg, V.: *J. Phys. A* **23**, L141(1990),
Affleck, I., *J. Phys.: Condens. Matter*, **2**, 405(1990).
- [37] Cardy, J.L.: *Nucl. Phys.*, **B270**, 186(1986).
- [38] den Nijs, M.: *J. Phys.*, **A17**, L295(1984),
Nienhuis, B.: *J. Stat. Phys.*, **94** 781(1984),
Dotsenko, V. and Fateev, V.A.: *Nucl. Phys.* **B210** 312(1984).
- [39] Belavin, A., Polyakov, A. and Zamolodchikov, A.: *Nucl. Phys.*, **B241**, 33(1984).
- [40] Friedan, D., Qiu, Z. and Shenkar, S.: *Phys. Lett.*, **15B**, 37(1985).
- [41] Alcaraz, F.C., Barber, M.N., Batchelor, M.T., Baxter, R.J. and Quispel, G.R.W.: *J. Phys.*,
A20, 6397(1987).
- [42] Martins, M.J.: *Phys. Lett. A*, **151**, 579(1990).

- [43] Alcaraz,F.C. and Martins,M.J.:*Phys. Rev. Lett.*, **63**, 708(1989).
- [44] Alcaraz,F.C., Grimm,M. and Rittenberg,V.:*Nucl. Phys.*, **B316**, 735(1989).
- [45] Warner,S.O., Batchelor,M.T. and Nienhuis,B.:*J. Phys. A*, **25**, 3077(1992).
- [46] Berker,R.N. and Kadanoff,L.:*J. Phys.*, **A13**, L259(1980).
- [47] Affleck,I.:*J. Phys.*, *C2*, 405(1990).
- [48] Wadati,M., Deguchi,T. and Akutsu,Y.:*Phys. Rep.*, **180**, 247(1989).
- [49] Birman,J. and Wenzl,H.:*Trans. Am. Math. Soc.*, **313**, 249(1989),
Murakami,J.:*Osaka J. Math.*, **24**, 745(1987).
- [50] Kauffman,L.:Pro. of the 13th Johns Hopkins Workshop on *Knots, Topology and Field Theory*, Firenze,
June 1989 (World Scientific).
- [51] Martin,P.:*"Potts model and related problems in statistical mechanics"*, World Scientific.
- [52] Kauffman,L.: unpublished notes.
- [53] Nienhuis,B.:*Phys. Rev. Lett.*, **49**, 1062(1982).